

Article

Study on the Impact of Design Factors of Piloti Forms on the Thermal Environment in Residential Quarters

Jinhan Li ¹, Xiaofang Shan ^{1,2,*} and Qinli Deng ^{1,2,*} 

¹ School of Civil Engineering and Architecture, Wuhan University of Technology, No. 122 Luoshi Road, Wuhan 430070, China; 11049732104702@whut.edu.cn (J.L.); xfshan@whut.edu.cn (X.S.)

² Hainan Institute, Wuhan University of Technology, No. 5 Chuangxin Road, Sanya 572024, China

* Correspondence: deng4213@whut.edu.cn

Abstract: According to piloti design, the outdoor thermal environment can be improved in cities with hot summer conditions. Taking Chinese cities with a hot summer and cold winter as the research object, this paper discusses the improvement of the outdoor thermal environment of residential districts in summer by considering piloti design factors. In this article, according to our investigation of piloti design in Wuhan, a basic model of the overhead layer in the Wuhan residential area is presented, along with the effects of different piloti ratios (0–80%), piloti heights (2–6 m), and greening rates (30–35%) on the outdoor thermal environment of buildings. The average air temperature and average wind speed at the pedestrian level are used as outdoor thermal environment indicators, the average PET is used as the outdoor thermal comfort indicator, and the comfort wind ratio is used as the outdoor wind comfort indicator. The results show that increasing the ratio of corridor columns has the greatest thermal comfort enhancement effect in the corridor area, and when the piloti ratio increases from 20% to 80%, the PET in piloti areas reduces by 2.926 °C. Improving the greening rate has the greatest thermal comfort enhancement effect in the passageway area, and when the greening rate increases from 20% to 80%, the PET in piloti areas reduces by 0.9 °C. Furthermore, the increases in both the piloti ratio and piloti height have an enhancement effect on the outdoor wind environment and wind comfort, with thresholds of a piloti ratio over 60% and a piloti height over 5 m. In contrast, the increase in the greening rate will deteriorate the outdoor wind environment and wind comfort. The conclusions of this study are of great significance for the planning and design of overhead layers in residential areas in hot and humid areas in summer.



Citation: Li, J.; Shan, X.; Deng, Q.

Study on the Impact of Design Factors of Piloti Forms on the Thermal Environment in Residential Quarters. *Buildings* **2024**, *14*, 1303. <https://doi.org/10.3390/buildings14051303>

Academic Editor: Eusebio Z.E. Conceição

Received: 25 March 2024

Revised: 28 April 2024

Accepted: 1 May 2024

Published: 5 May 2024



Copyright: © 2024 by the authors. Licensee MDPI, Basel, Switzerland. This article is an open access article distributed under the terms and conditions of the Creative Commons Attribution (CC BY) license (<https://creativecommons.org/licenses/by/4.0/>).

Keywords: outdoor thermal environment; piloti design; greening rate; residential quarters; human thermal comfort

1. Introduction

A comfortable outdoor environment leads to a greater willingness of city dwellers to engage in outdoor activities, including walks, cycling, and outdoor ball games, which offers people a greater sense of well-being. At the same time, outdoor activities can also reduce energy consumption in built-up areas [1]. However, in most parts of China, where summers are always hot, outdoor thermal comfort is often affected by unfavorable factors, such as strong solar radiation and wind conditions, as well as high temperatures from the urban heat island effect [2,3]. At the same time, land use has changed significantly [4,5]. Early studies have shown that the loss of green spaces and the application of paving, together with a significant increase in anthropogenic heat released, have affected the urban climate, leading to severe environmental degradation and significantly increasing the ecological footprint of the city [6–8]. Because of their growing populations, cities require large amounts of energy to function properly. In fact, urban dwellers consume more than 75% of the total energy due to activities carried out in the urban environment [9,10]. Relevant studies have shown that the heat island effect in Wuhan is significant and that there is a strong positive correlation between the number of people in the urban area of Wuhan and the heat island

effect [11]. At the same time, the population of Wuhan has increased by 2.54 million people from 2011 to 2021, that is, by nearly 20%. The rising population trend will continue in China's urbanization process [12], which will undoubtedly have a negative impact on the thermal environment and thermal comfort in Wuhan, and the duration of extreme high temperatures will also increase significantly in the future.

In recent years, a variety of strategies have been used to improve the outdoor thermal environment and thermal comfort in cities. One of the strategies is to use pilotis to provide shading for building areas and affect natural ventilation, which can facilitate air circulation within the building area, thereby improving wind comfort and average wind speeds [13–19]. Piloti design has also been considered as an effective means of cooling. Studies on the outdoor thermal environment of buildings with different piloti design variables have mainly focused on the piloti rate, the height of the piloti core, and the position of the piloti setting relative to the buildings [20]. Xi et al. [21,22] used questionnaires and numerical simulations to calculate the thermal sensation and thermal comfort in the campus area of Guangzhou on 14 July and 15 July in summer, recording data changes in building pedestrian height SET* at piloti ratios of 0–100%. The results showed that an increase in the piloti ratio could improve the thermal comfort in spaces sheltered by the pilotis, and that when the piloti ratio was 100%, the SET* in this space could satisfy the human body limit. Zhou [23] investigated the outdoor thermal environment of Wuhan in summer (July) and winter (January). Based on the optimal location of the piloti arrangement (both ends), the relationship between the piloti ratio and the outdoor wind environment was investigated. Their results showed that the wind speed increased with the growing piloti ratio in summer, and that it slightly changed in winter. Thus, it was surmised that the piloti ratio should be between 12% and 38% to avoid discomfort caused by wind in winter. Chen et al. [24] simulated the influence of indoor ventilation on the outdoor thermal environment of a campus building in Guangzhou, and they researched the improvement of the outdoor thermal environment in the campus area with different piloti heights and piloti ratios.

Apart from buildings, trees are another major determinant of the thermal environment in residential areas, with effects through shading, evapotranspiration, and increased albedo [25–27]. Canopies of trees can act as shading like buildings to block solar radiation and thus have a reducing effect on the surface temperature as well as the air temperature in residential areas [28]. At the same time, evapotranspiration from trees can reduce sensible heat and increase the latent heat flux into the air [29,30]. In addition, since the albedo of trees is higher than that of built-up areas, more trees can reflect more solar radiation, thus lowering the surface temperature [31]. In residential areas, where buildings are usually planned or constructed first, trees are considered a great method to mitigate the effects of the thermal environment. Therefore, it is necessary to evaluate the ability of trees to influence the thermal environment with appropriate methods. Several previous studies have been conducted on the effectiveness of trees in improving the thermal environment in residential areas during the summer and have confirmed that trees can improve the thermal environment of buildings to a certain extent [32–34]. However, trees also have a negative effect on the wind speed in the area to a certain extent, which is contrary to the design concept of increasing wind speed for piloti design. The effect of the tree greening rate on the thermal environment with respect to the piloti building area is yet to be investigated.

Most of the existing studies on the thermal environment of piloti buildings have failed to consider the influence of complex urban blocks on the thermal environment of buildings. Most of them have focused on a single block scale, where the buildings are replaced by ideal blocks, or purely on a single building, without considering the role of vegetation and the influence of the subsurface on the thermal environment. In addition, there is a lack of research on thermal comfort at the pedestrian level in residential quarters based on piloti design variables (Table 1). Furthermore, there is a lack of qualitative and quantitative studies on greening that study the effect of the greening rate on outdoor thermal comfort in piloti residential quarters.

Therefore, in order to address the research gaps in regard to the thermal environmental aspects of elevated buildings and the lack of studies on greenery settings, efforts have been made to diversify the scope of research in this area. This article presents a basic model of piloti residential quarters in Wuhan. Three design variables are considered: two piloti design variables, i.e., piloti ratio and piloti height, to analyze the impact of piloti installations on the outdoor thermal environment residentially in terms of changes caused by changes in these two design variables; and one overall architectural design variable, i.e., the greening rate of the residential area, to qualitatively analyze outdoor thermal comfort by increasing greenness in piloti residential quarters and to explore whether a threshold exists. A total of 15 models were established for comparison, to derive the effects of each design variable on the thermal environment of piloti buildings. This study offers a reference for the design of piloti buildings in hot and humid areas, along with assistance for urban design planners seeking to mitigate the increasingly severe heat island effect.

2. Methods

2.1. Study Area

Located in central China, Wuhan is at $30^{\circ}35'$ north latitude, $114^{\circ}17'$ east longitude, standing at 23 m above sea level. It is the fifth largest city in China, with about 13.74 million urban residents. Wuhan has a typical subtropical monsoon climate with hot summers and cold winters. Summer extends from June to September, with July and August being the two hottest months. Wuhan's urban area is sweltering in summer, with daytime temperatures often around 37°C and nighttime temperatures around 30°C , with an extreme maximum of 41.3°C . The wind speed is low in summer, with an average wind speed of about 1 m/s from the southwest. Such meteorological conditions may exacerbate people's feeling of high temperatures and make the heat more unbearable. In contrast, winter is a cold and dry season from December to February, with an average temperature of about 3°C . Wind from the north is more common, with an average wind speed of 4–5 m per second. Wuhan is in the eastern part of the Jiangnan Plain, with 166 lakes of various sizes scattered throughout the city, and the average relative humidity of the air is high at about 73–77% throughout the year (Figure 1).

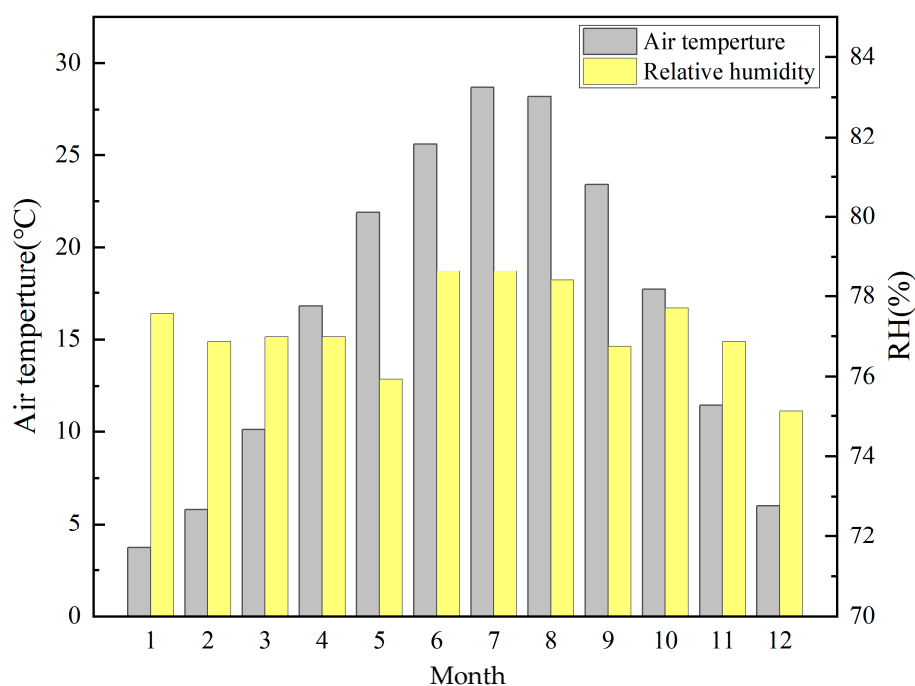


Figure 1. Monthly average temperature and humidity in Wuhan. Source <https://xihe-energy.com/> (assessed on 4 May 2022).

2.2. Research on the Status of Piloti Residential Quarters in Wuhan City

The purpose of this study was to facilitate an understanding of the status quo of the construction of pilotis in Wuhan's residential areas, and to statistically analyze the form, layout, and use of the pilotis. This study adopted an offline research method to gather statistics on the piloti residential districts in Wuhan's various central urban areas, and the specific data of the research are shown in Table 2. Between the 19 residential quarters with pilotis (Figure 2), the following common features were found in Wuhan:

1. The piloti ratio is below 50%.
2. Most pilotis are located on both sides of the buildings; only individual buildings in individual districts use middle pilotis due to the topography and orientation of these buildings. In those districts where there is a single middle-piloti building, most of the buildings are elevated at both ends.
3. The greening rate is less than 50% but higher than 25%.
4. The piloti height is between 2 and 6.5 m: when it is less than 2.5 m, piloti areas act as underground car parks; and only a small number are more than 5.5 m. Based on the status quo of the pilotis in Wuhan residential districts, the ideal district model was extracted and can be used as a substitute: a 40% piloti ratio, 30% greening rate, 4 m piloti height, and parallel rows and columns as the building layout.

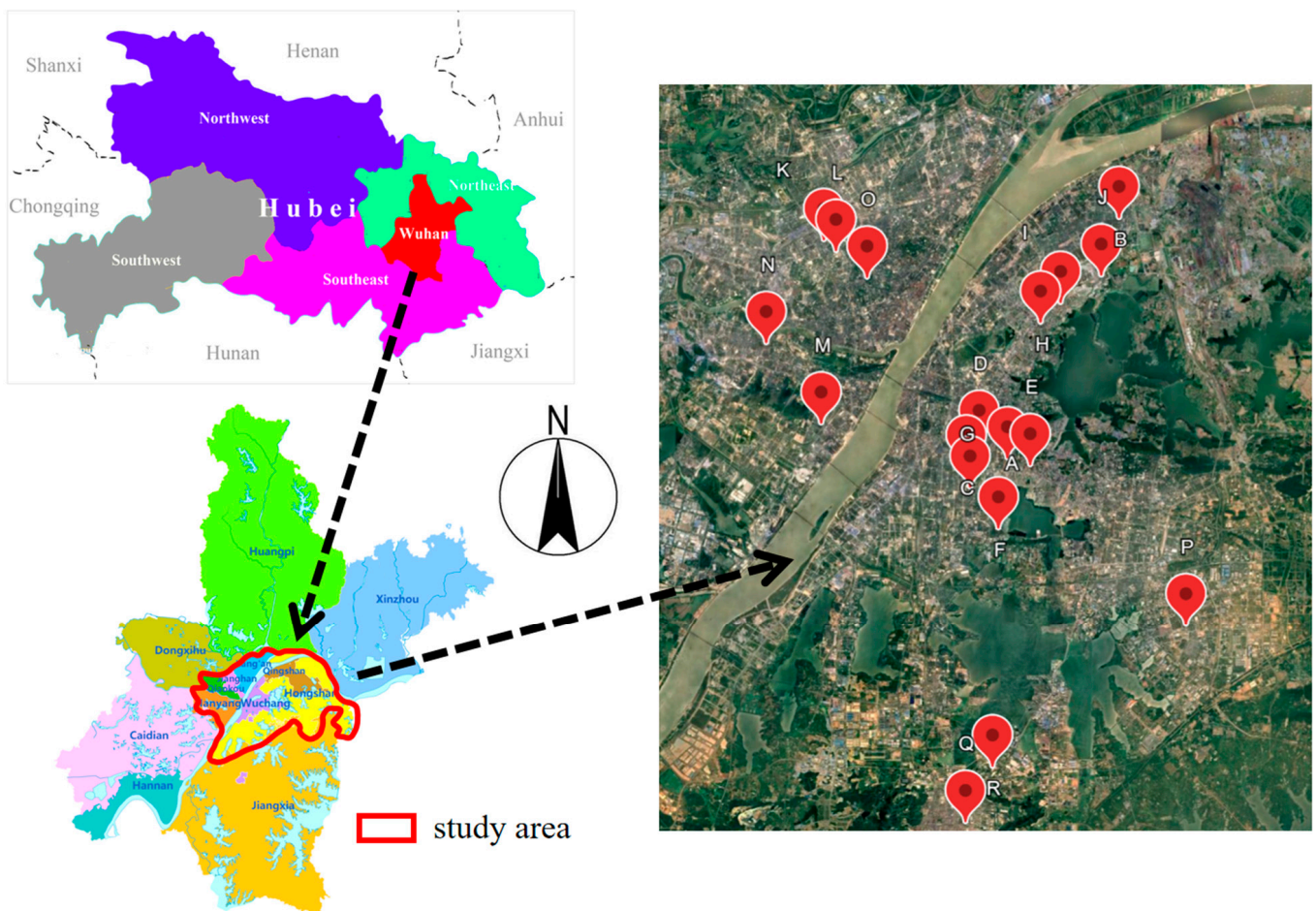


Figure 2. Distribution map of the research community.

Table 1. Difference between selected piloti building research papers and this study.

References	Content of Research	Differences from this Research
[13]	Study of the impact of piloti ratio, piloti height, and geometry on the wind environment	No consideration of the thermal environment, underpinning, or greening
[15]	Impact of piloti ratio and wind direction on the wind environment	No consideration of the thermal environment, underpinning, or greening
[18]	Study on the impact of piloti buildings with different piloti heights and widths on the wind environment	No consideration of the impact on the thermal environment
[21]	Study on the impact of buildings with different piloti ratios on the outdoor thermal environment	No categorization of the underlay and no consideration of the impact of greening
[23]	Analysis of the cooling and thermal environment improvement effects of piloti buildings through measured methods	Using measured methods while not considering underpinning or greening

2.3. Assessment Methodology

In this study, the physiological equivalent temperature (PET) [35] was used as the thermal environment assessment index. The PET is calculated based on environmental parameters such as air temperature, wind speed, mean radiant temperature, relative humidity, clothing thermal resistance, and activity level. The personal parameters of the PET are set as male, 35 years old, height 1.75 m, weight 75 kg, physiological metabolism 80 W, labor metabolism 85 W, thermal resistance value 0.31, and height 1.5 m above the ground.

A comfortable wind ratio is used as the evaluation standard of outdoor wind comfort. The comfortable wind ratio is the area occupied by comfortable wind in the target area divided by the area of the target area, and the evaluation criteria of comfort wind are shown in Table 3 [36].

Table 2. Basic information table of piloti in residential quarters of Wuhan.

Residential Quarter	Greening Rate	Piloti Height	Piloti Arrangement
A	35%	5 m	at the two ends of the building
B	15%	4.2 m	at the two ends of the building
C	28%	6.5 m	at the two ends of the building
D	30%	3.9 m	at the two ends of the building
E	28%	4.4 m	in the middle of the building
F	30%	4.5 m	at the two ends of the building
G	35%	5.4 m	at the two ends of the building
H	36%	2 m	at the two ends of the building
I	35%	4.6 m	at the two ends of the building
J	35%	2.6 m	at one end of the building
K	35%	3.9 m	at the two ends of the building
L	40%	2.6 m	at the two ends of the building
M	30%	4.2 m	in the middle of the building
N	30%	2.6 m	at the two ends of the building
O	35%	3.9 m	at the two ends of the building
P	35%	5.2 m	at the two ends of the building
Q	35%	2.8 m	at the two ends of the building
R	30%	3.4 m	at the two ends of the building
S	38%	3.2 m	at the two ends of the building

2.4. Envi-Met Software Thermal Environment Validation

2.4.1. Introduction of the Validation Case

Envi-met validation is carried out using Li's measurements in the Xixiu Village neighborhood of South China University of Technology [37]. This is located in the western district of the university and forms a faculty and staff residential neighborhood. The whole community covers an area of nearly 24,000 square meters, with a building density of 32%, a greening rate of 33%, and a row-type building layout. Between the 5th and 7th faculty flats is the central garden, covering an area of about 1086 m², equipped with slides and other activity facilities. Between the 12th faculty flat that is near the entrance to the community and adjacent to the western student dormitory and 13th faculty flats is a space raised at about 3.2 m, of which the lower part is a garage and the upper part is the pavement. Measurement point A1 is between the 12th and 13th buildings in Xixiu Village, with no shade; A5 is between the 2nd and 3rd buildings under mango trees, with relatively dense shade; and A7 is between the 3rd and 4th buildings under street trees, with sparse shade. The distribution of measurement points in the model is shown in Figure 3.

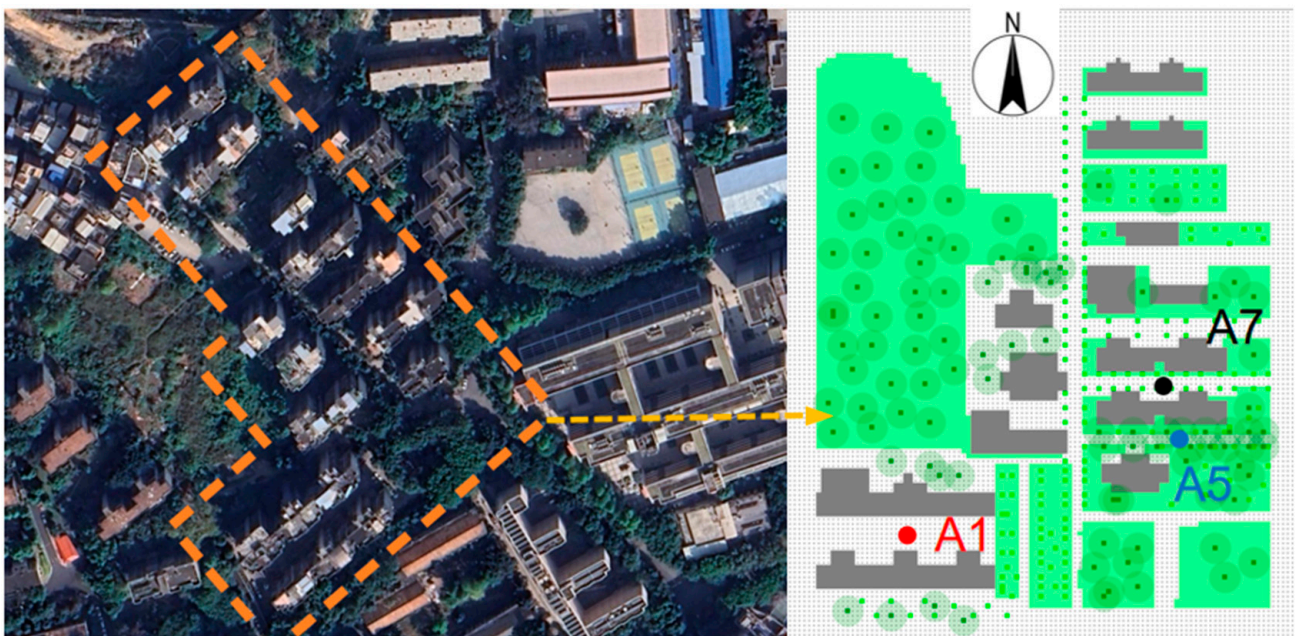


Figure 3. Distribution of measurement points in the Xixiu District cluster.

2.4.2. Validation Results

We compared the measured air temperature and relative humidity data of three measurement points [38], A1, A5, and A7, in the Xixiu Village community at a pedestrian-level height of 1.5 m with the simulated data from the Envi-met 5.5.1. The evaluation indexes commonly used in the validation of thermal environmental simulation are root mean square error (RMSE), mean absolute error (MAE), mean absolute percentage error (MAPE), and Willmott's index of agreement (d) [39], and the specific calculation methods of each index are as follows:

$$\text{RMSE} = \sqrt{\frac{1}{n} \sum_{i=1}^n (P_i - O_i)^2} \quad (1)$$

$$\text{MAE} = \frac{1}{n} \sum_{i=1}^n |P_i - O_i| \quad (2)$$

$$\text{MBE} = \frac{1}{n} \sum_{i=1}^n \frac{P_i - O_i}{O_i} \quad (3)$$

$$d = 1 - \frac{\sum_{i=1}^n |O_i - P_i|}{\sum_{i=1}^n (|P_i - \hat{O}| + |O_i - \hat{O}|)} \quad (4)$$

In the formulas above, “ P_i ” represents simulation data, “ O_i ” represents measured data, “ \hat{O} ” is the average value, and “ n ” is the number of measurement points. The comparison results are shown in Figure 4. Envi-met shows a better simulation of air temperature than relative humidity and is also better during the day than at night. Meanwhile, when comparing the data agreement of the three different measurement points, it can be found that the simulation effect of point A1 is the best, which is due to the influence of vegetation at points A5 and A7 (Table 4). Therefore, the consistency for temperature and relative humidity is not as good as that of point A1. The consistency between the simulated and measured values of temperature and relative humidity at 1.5 m for the three groups of points is acceptable ($D > 0.6$). Based on validation and comparison results above, it can be concluded that Envi-met version 5.5.1 offers a reasonable prediction of the thermal environment in a complex residential area in hot and humid environments.

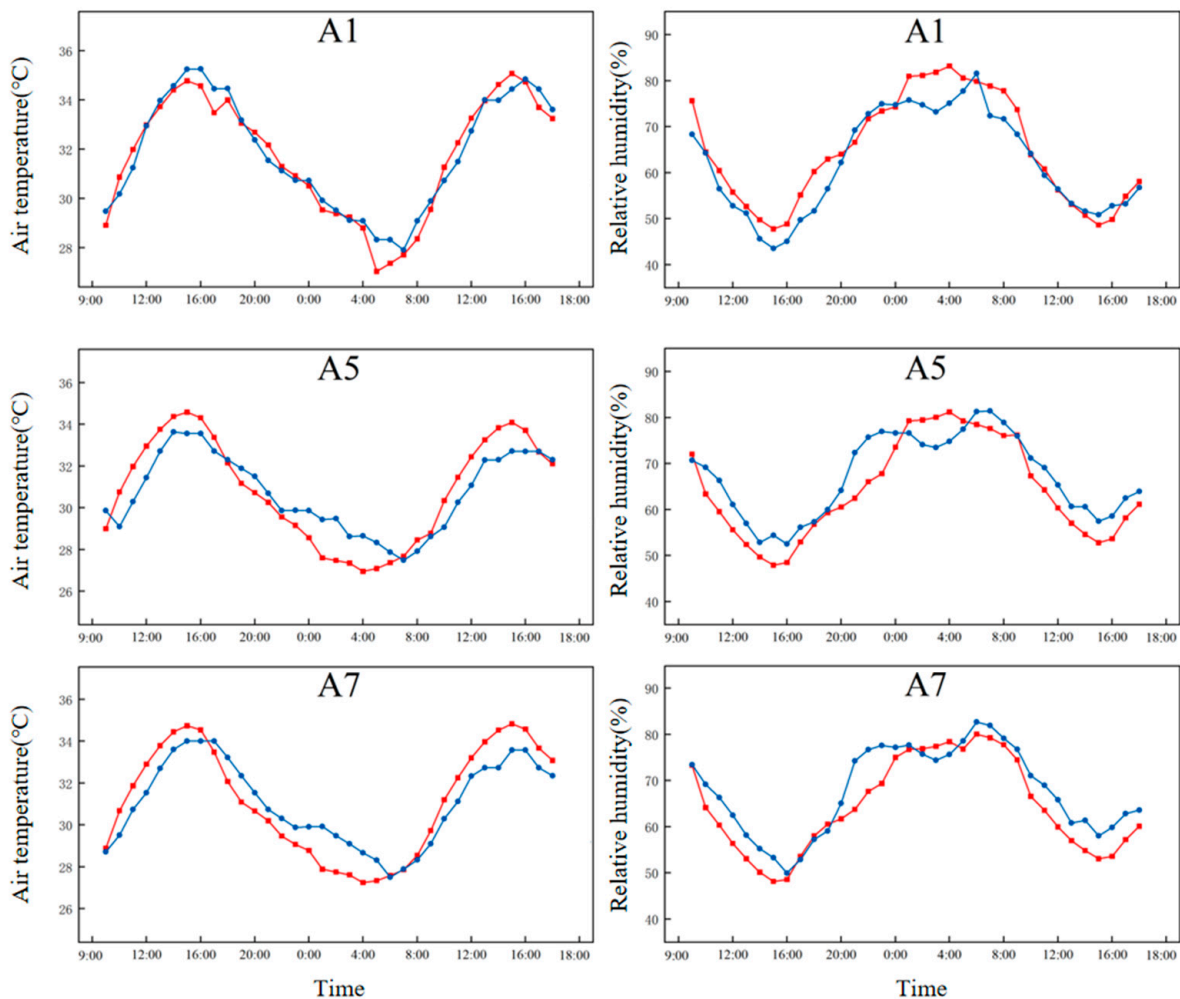


Figure 4. Comparison of the simulated and measured results for air temperature and relative humidity. (The blue curve represents simulated values, and the red curve represents measured values).

2.5. Analysis Model and Cases

The analytical model of this study was formed with reference to the research on the current situation of piloti buildings in Wuhan, as shown in Figure 5. The overall model is a row-type building cluster consisting of 7 rows and 6 columns with a total of 42 single buildings, and the size of the whole computational domain is 456 m (X) × 484 m (Y) × 220 m

(Z). The buildings are separated by 36 m from left to right and 16 m from front to back, and the building height is 65 m. The target area is the six buildings in the center of the cluster, which are used to remove the uncertainty brought about by the influence of the complex urban block on the wind and thermal environments in the study area [33]. The dimensions of the target area are 136 m (X) × 168 m (Y) and the dimensions of the aisle area are 8 m (X) × 168 m (Y). The boundary condition settings of the model are shown in Table 5. The overall greening rate of the building area varies in the range of 30–50%, in which the ratio of the area of trees, shrubs, and lawns remains unchanged. The variation range of piloti height is 2–6 m. A total of 15 calculation cases were set up in this study with differences in greening rate, piloti ratio, and height (Table 6).

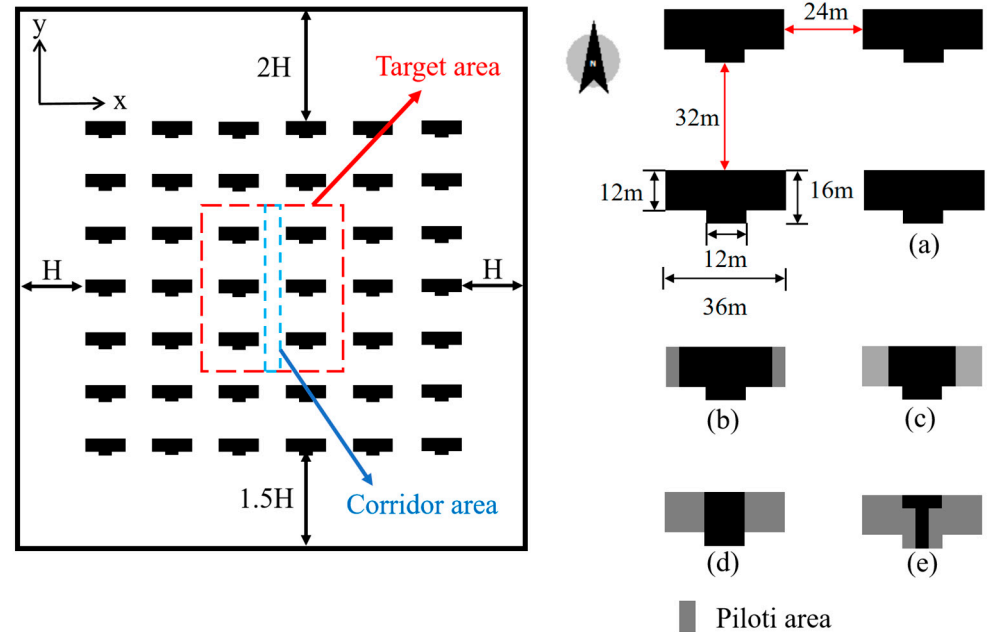


Figure 5. Architectural layout and building model piloti diagram. (a–e) are schematic diagrams of piloti ratios ranging from 0% to 80%. The gray areas represent piloti spaces.

Table 3. Evaluation principle of velocity considering temperature influence.

Evaluation Range	Temperature Range (°C)		
	<10	10~25	>25
Range of breezes that cause thermal discomfort in the human body (m/s)	—	—	<0.7
Human comfortable wind speed range (m/s)	<1.3	<1.5	0.7~1.7
Excessive range between comfortable and uncomfortable winds (m/s)	1.3~2.0	1.5~2.3	1.7~2.9
Range of strong winds that cause human discomfort (m/s)	>2.0	>2.3	>2.9

Table 4. Index values of air temperature and relative humidity at the measuring points.

Measuring point	RMSE	MAE	MBE	D
A1 (T _a)	0.538	0.442	−0.100	0.89
A5 (T _a)	1.1	0.962	0.14	0.64
A7 (T _a)	1.064	0.959	0.087	0.712
A1 (RH)	4.41	3.54	0.058	0.823
A5 (RH)	5.002	4.416	−2.986	0.669
A7 (RH)	4.7	3.985	−3.398	0.74

Table 5. Envi-met parameter setting.

Parameter Setting		
Location	Wuhan Roughness	(114.30, 30.5) 0.1
Time	Start time Total simulation time (h) Pre-run time	7.31 00:00 21 h 7 h
Building Parameter	Wall heat transfer coefficient ($w/m^2 \cdot k$) Roof heat transfer coefficient ($w/m^2 \cdot k$) Wall reflectance (%) Roof reflectance (%)	1.7 2.2 0.3 0.15
Vegetation	Lawn Hedge Tree	XY (grass 50 cm aver. dens.) H2 (Hedge 2 m dens.) T1 (Tree 10 m dens.)
Underlying surface	Brick road (red stones) Brick road (yellow stones) Dark concrete pavement Asphalt road Sandy loam	reflectance: 0.3; emissivity: 0.9 reflectance: 0.4; emissivity: 0.9 reflectance: 0.2; emissivity: 0.9 reflectance: 0.12; emissivity: 0.9 reflectance: 0.2; emissivity: 0.9
Grid setting	Grid size Number of grids Number of nested grids Size of the computational domain	4 m(X) \times 4 m(Y) \times 3 m(Z) 114(X) \times 121(Y) \times 25(Z) 6 456 m(X) \times 484 m(Y) \times 220 m(Z)

Table 6. Analysis cases.

Case	Floor Space (m ²)	Piloti Area Space (m ²)	Piloti Ratio	Greening Rate	Piloti Area Height (m)
1	480	0	0%	30%	4 m
2	480	96	20%	30%	4 m
3	480	192	40%	30%	4 m
4	480	288	60%	30%	4 m
5	480	384	80%	30%	4 m
6	480	192	40%	30%	2 m
7	480	192	40%	30%	3 m
8	480	192	40%	30%	4 m
9	480	192	40%	30%	5 m
10	480	192	40%	30%	6 m
11	480	192	40%	30%	4 m
12	480	192	40%	35%	4 m
13	480	192	40%	40%	4 m
14	480	192	40%	45%	4 m
15	480	192	40%	50%	4 m

3. Results and Analysis

This study examined the effects of piloti ratio, piloti height, and the overall greenness of piloti residential quarters on the thermal environment and thermal comfort of the piloti residential area. The results related to changes in mean air temperature (T_a), mean radiant temperature (MRT), mean physiological equivalent temperature (PET), mean wind speed, and comfort wind ratio at the pedestrian level. All of those are discussed herein for a comprehensive and accurate analysis and evaluation of the thermal environment. During the hot summer months, the main activity areas of pedestrians and occupants walking in residential neighborhoods are mainly in the aisles between two buildings as well as in the piloti areas (Figure 5). Therefore, this study analyzed the aisle and piloti areas along with the overall thermal environment of the target area. Three time points, 8:00, 14:00, and 18:00, were selected for analysis in order to understand the changes in the thermal environment

during the day. Terms and abbreviations used in this paper can be found in Appendix A and Vector wind speed cloud chart can be found in Appendix B.

3.1. Effect of Piloti Ratio on the Outdoor Thermal Environment and Thermal Comfort in Piloti Residential Quarters

3.1.1. Air Temperature

The air temperature (T_a) at the pedestrian level for buildings with different piloti rates at the 8:00, 14:00, and 18:00 points are shown in Figure 6. It can be concluded that the 14:00 period has the greatest cooling. Meanwhile, the thermal environment is also in the worst condition at this time, because it is at the hottest time of the day in summer in Wuhan. The average air temperature of the target area decreases with the rise in piloti ratio. When the piloti rate is from 0% to 20%, it decreases the most; while from 60% to 80%, it decreases the least. The average air temperature decreases by $0.327\text{ }^{\circ}\text{C}$ at an 80% piloti ratio compared to the temperature at a 0% piloti ratio, and the box plot shows that the upper limit of the air temperature in the area also decreases as the piloti ratio increases.

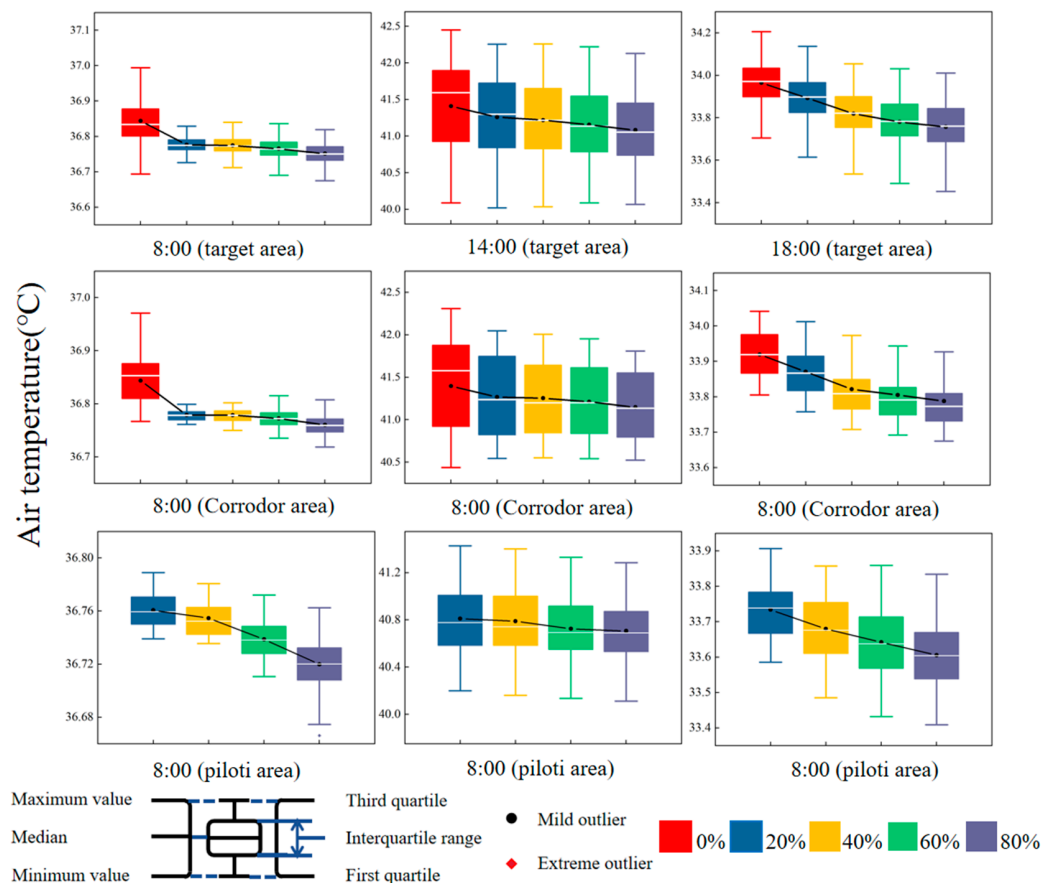


Figure 6. Average air temperature at 1.5 m height in the study area (target area, aisle area, piloti area) for buildings with different piloti ratios (0–80%) at different times of the day: morning (8:00), midday (14:00), nightfall (18:00).

In the aisle area, the increase in piloti ratio also has an effect of decreasing the average air temperature at the pedestrian level. The most significant decrease in temperature is observed from a 0% to 20% piloti ratio, which indicates that the increase in piloti ratio leads to a decrease in the total amount of solar radiation reflected by the buildings into the aisle area, thus causing a certain decrease in the air temperature in the aisle area. The maximum temperature drop still occurs at 14:00. The average air temperatures in the aisle area decrease by $0.126\text{ }^{\circ}\text{C}$, $0.14\text{ }^{\circ}\text{C}$, $0.181\text{ }^{\circ}\text{C}$, and $0.244\text{ }^{\circ}\text{C}$ for the 20% to 80% piloti ratios compared to the no piloti case. The smallest temperature drop is at 18:00.

In the piloti area, the increase in the piloti ratio has a limited effect on the air temperature reduction in the piloti region. Different from the other two regions, the cooling in the piloti area is greater at 8:00 than at 14:00. Because the sun's angle is lower in the morning, and buildings with a low piloti ratio are exposed to direct sunlight, while buildings with a high piloti ratio are not exposed to direct sunlight in some areas. At 14:00, since the sun's angle is higher, the amount of radiation received by piloti areas with different overhead ratios is the same. At 14:00, the average air temperature drops in the piloti area of the 20% piloti ratio case are only 0.021 °C, 0.086 °C, and 0.104 °C when compared with the 40–80% piloti ratio cases.

An increase in piloti ratio has a cooling effect on the overall air temperature at the pedestrian level in the target area. This cooling effect is mainly achieved through the increase in the shading area caused by the increase in the piloti ratio, thus lowering the overall average air temperature. In the aisle area, although a piloti does not provide shading, it can still reduce the average air temperature to a certain extent. For the piloti area, the increase in the piloti ratio does not have a significant effect on the average air temperature, which only decreases slightly.

3.1.2. Wind Speed and Comfort Wind Ratio

The average wind speeds in the target area of buildings with different piloti ratios are shown in Figure 7, where the average wind speeds at 8:00 and 18:00 are increasing with the increase in piloti ratio, while the average wind speed at 14:00 is decreasing with the increase in piloti ratio. The average wind speed in the target area is very low owing to the obstruction provided by external buildings, so wind speed variation caused by the change in the piloti ratio is not observed. At 14:00, when the variation in wind speed is at its maximum, the wind speeds of the buildings with 20–80% piloti ratios increase by 0.129 m/s, 0.147 m/s, 0.180 m/s, and 0.220 m/s, respectively, compared to buildings without pilotis, which has a very limited effect on the comfort of the outdoor thermal environment.

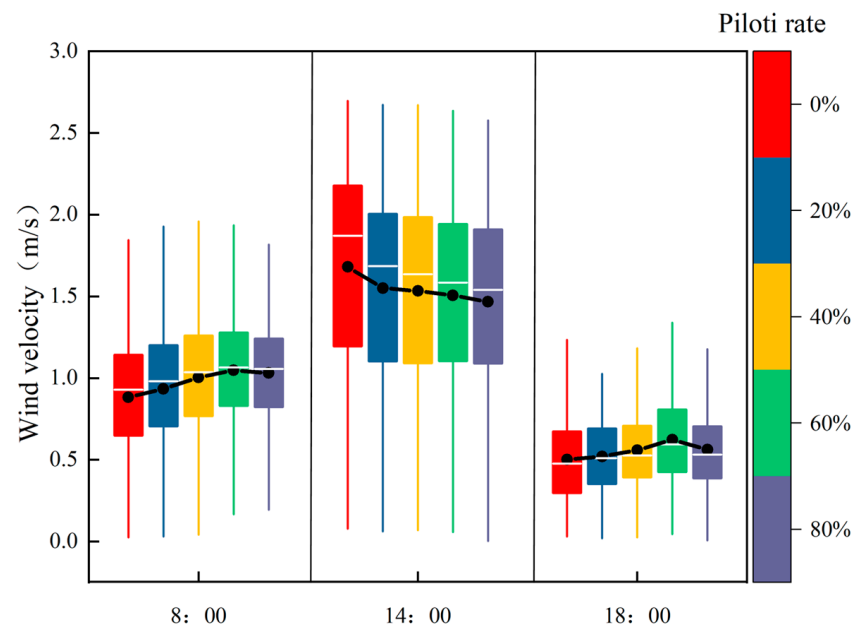


Figure 7. Wind speeds in the target area at 8:00, 14:00, and 18:00.(Different piloti ratio model)

A histogram of the proportion of comfortable wind points at the pedestrian level for different overhead rates in the target area is shown in Figure 8. In the target area, the proportion of comfortable wind increases with the increase in piloti ratio. This indicates that an increase in piloti ratio can increase the proportion of comfortable wind in the target area. When the piloti ratio is from 0% to 60%, the proportion of comfortable wind increases

faster, but when the piloti ratio is higher than 60%, it increases slowly, and it starts to decrease at 18:00.

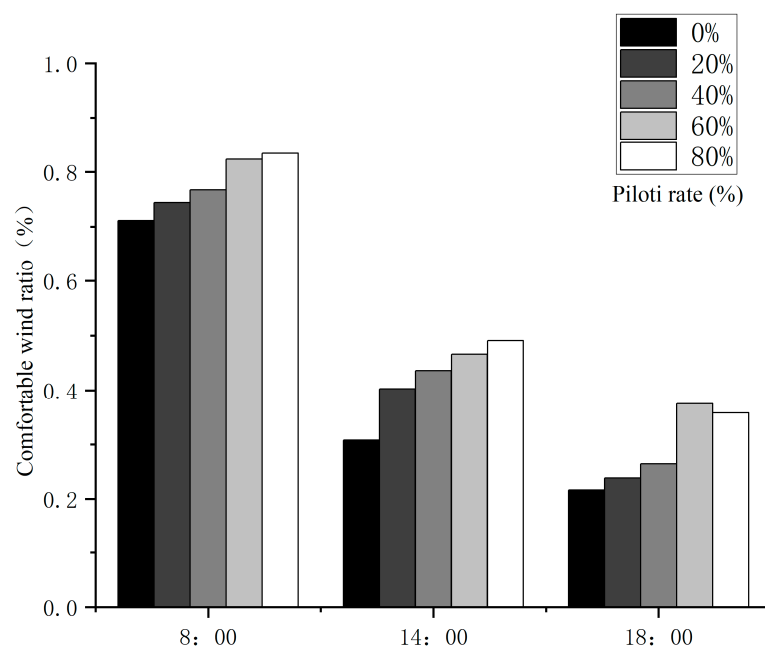


Figure 8. Schematic representation of the proportions of comfortable winds at 8:00, 14:00, and 18:00 for buildings with different piloti ratios in the target area.

The increase in piloti ratio does not have a significant effect on the variation in pedestrian average wind speed in the target area, due to changes in wind direction. Moreover, the increase in the piloti ratio improves the proportion of comfortable wind in the target area, and its influence is reflected most obviously when piloti ratio is from 0% to 60%. When the piloti ratio is between 60% and 80%, an increase in the piloti ratio can bring a decrease in the proportion of comfortable winds. Therefore, the wind environment and wind comfort in the target area can be improved when the piloti ratio does not exceed 60%.

3.1.3. PET

Box plots of PET at three time points for buildings with different greenness rates are shown in Figure 9. The decrease in PET is greater compared to the air temperature because the PET is significantly correlated with the mean radiant temperature, which decreases significantly. The average radiant temperatures for the three regions at 14:00 are shown in Figure 10. At 8:00, the PET decreases by 0.424 °C, 0.039 °C, and 0.357 °C per a 20% increase in piloti ratio for the target, aisle, and piloti area, respectively. The aisle area between buildings is less affected by the piloti setting, so the PET in the aisle area decreases less in comparison.

Like air temperature, the largest PET drop also occurs at 14:00, when for every 20% increase in piloti ratio, the PET decreases by 0.546 °C, 0.029 °C, and 0.946 °C in the target, aisle, and piloti areas, respectively. At 18:00, the average PET of the target region as well as the aisle region change very little. Moreover, the average PET in the aisle area increases as the piloti ratio increases from 0% to 60%. In the piloti area, the average PET decreases by about 0.431 °C for each 20% increase in the piloti ratio.

It can be concluded by analyzing the three study areas of the building model with different piloti ratios that an increase in the piloti ratio reduces the average PET in the three regions, resulting in better pedestrian thermal comfort. In the target and piloti areas, a decrease in piloti ratio can reduce the lower limit of PET, while in the aisle area, it can raise that lower limit.

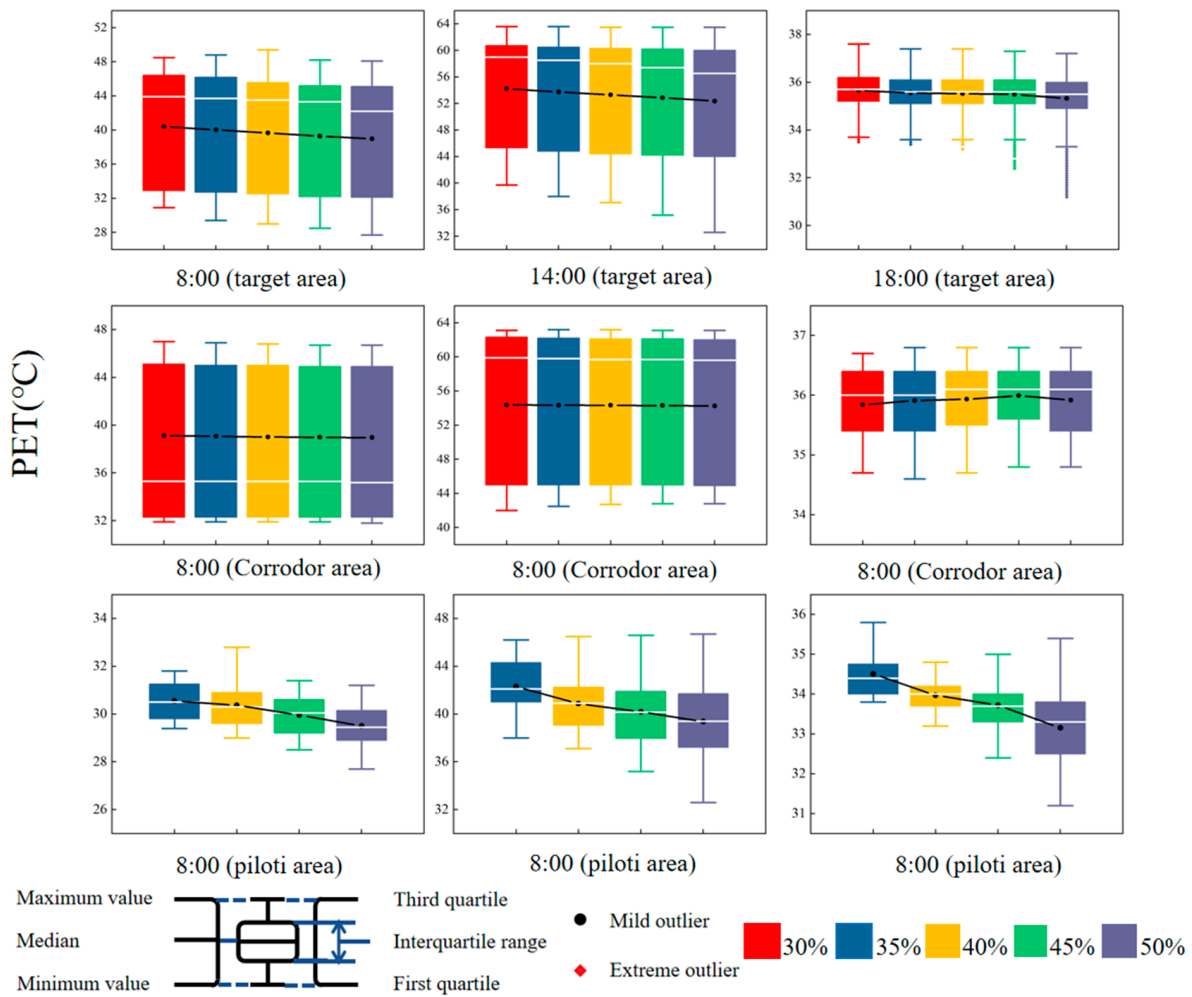


Figure 9. The 1.5 m height PET of the study area (target area, aisle area, piloti area) at different times of the day for buildings with different piloti ratios (0–80%): morning (8:00), midday (14:00), nightfall (18:00).

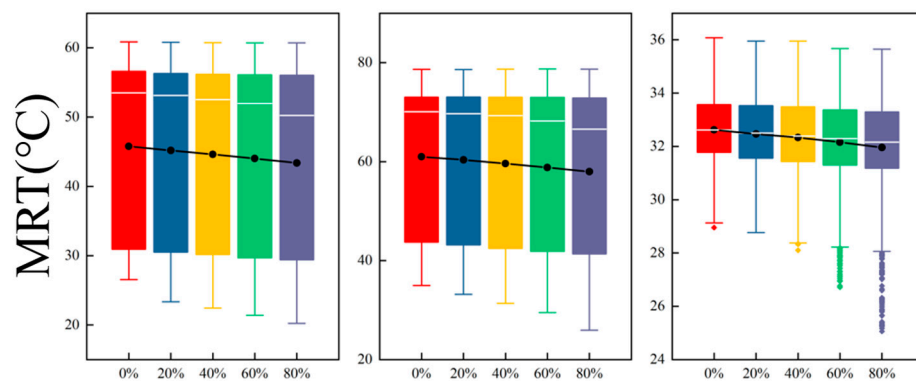


Figure 10. MRTs of target areas for buildings with different piloti ratios (8:00, 14:00, 18:00).

3.2. Analysis of the Impact of Piloti Height on the Outdoor Thermal Environment of Piloti Residential Areas

3.2.1. Air Temperature

The air temperatures (T_a) in the target areas of buildings with different piloti heights at 8:00, 14:00k, and 18:00 are shown in Figure 11. At 8:00, the overall temperature of the target area has a decreasing trend to an extent as the piloti height increases from 2 m to

4 m. At 14:00 and 18:00, the average temperature of the target area increases gradually as the piloti height increases. At 14:00, when the height of the piloti rises to 6 m, the average temperature of the pedestrian level rises by $0.231\text{ }^{\circ}\text{C}$ when compared with that when the piloti height is 2 m. The main reason for the increasing temperature is that the elevation of the piloti height increases solar radiation. Accordingly, the average MRTs of the target areas of the buildings with piloti heights of 3–6 m rise by 0.062 , 0.373 , 0.546 , and $0.677\text{ }^{\circ}\text{C}$ at 14:00 compared to that for buildings of 2 m, respectively.

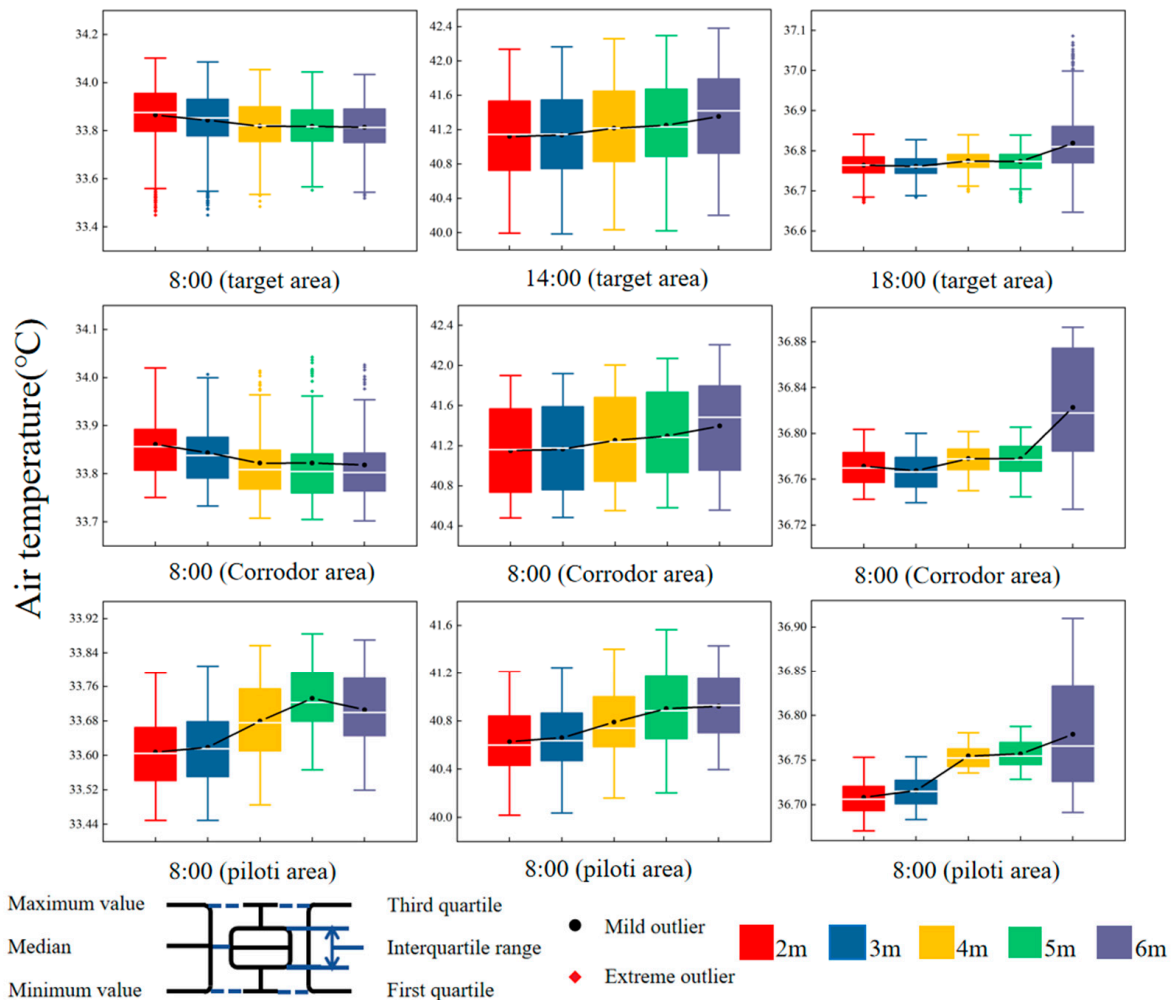


Figure 11. Average air temperature at 1.5 m height in the study area (target area, aisle area, piloti area) for buildings with different piloti heights (2–6 m) at different times of the day: morning (8:00), midday (14:00), nightfall (18:00).

In the aisle area, the trend and magnitude of change in the average pedestrian-level temperature are consistent with those in the target area. The average T_{mrt} in the aisle region is essentially unchanged at all three time points, indicating that the increase in piloti height does not affect the average radiant temperature in the aisle region.

In the piloti area, the average air temperature at all three time points increases with the increase in piloti height, and the temperature has the largest rise. Furthermore, the increasing piloti height has a greater effect on the average radiant temperature in the piloti area. At 14:00, the average radiant temperatures in the piloti areas of buildings with piloti heights of 2–6 m are $30.772\text{ }^{\circ}\text{C}$, $32.336\text{ }^{\circ}\text{C}$, $37.29\text{ }^{\circ}\text{C}$, $41.278\text{ }^{\circ}\text{C}$, and $42.761\text{ }^{\circ}\text{C}$, respectively. The increase in the average radiant temperature is fairly significant: compared to a piloti height of 2 m, the average radiant temperature of buildings with a height of 6 m increases by $4\text{ }^{\circ}\text{C}$.

3.2.2. Wind Speed and Comfort Air Ratio

The wind speed simulation results in Figure 12 show that the average wind speed at the pedestrian level at 8:00 and 18:00 becomes larger as the piloti height increases. The change in wind speed at 8:00 is the largest, and the average wind speed essentially shows a strong linear relationship with the height of the piloti area. For every 1 m increase in the piloti area, the wind speed changes by about 0.03 m/s. At 14:00 and 18:00, the average wind speeds in the target area of buildings with a piloti height of 6 m are lower than those with buildings at 5 m. The average wind speed in the target area of the buildings with a height of 6 m is higher than that with buildings at 5 m. As shown in Figure 13, the presence of a reverse wind region in the target area leads to a strange phenomenon where the average wind speed at a piloti height of 6 m is lower than that at a piloti height of 5 m, because the reverse wind return reduces the average wind speed in the target area. The proportions of average comfortable wind for different piloti heights in the target area are shown in Figure 14. When the piloti height changes from 2 m to 5 m, the proportions of comfort wind at all three time points increase to an extent. Compared to the change in the proportion of comfortable wind brought about by changes in the piloti ratio, the change in the proportion of comfortable wind resulting from increasing the piloti height is smaller. For instance, at 8:00 in the morning, although there is a slight increase in the average wind speed, the proportion of comfortable breeze remains largely unchanged. This is because the wind speeds at 8:00 in the morning fall within the comfortable breeze range (0.7–1.7 m/s). Similar to the change in average wind speed, the proportion of comfortable wind speed decreases when the piloti height increases to 6 m from 5 m.

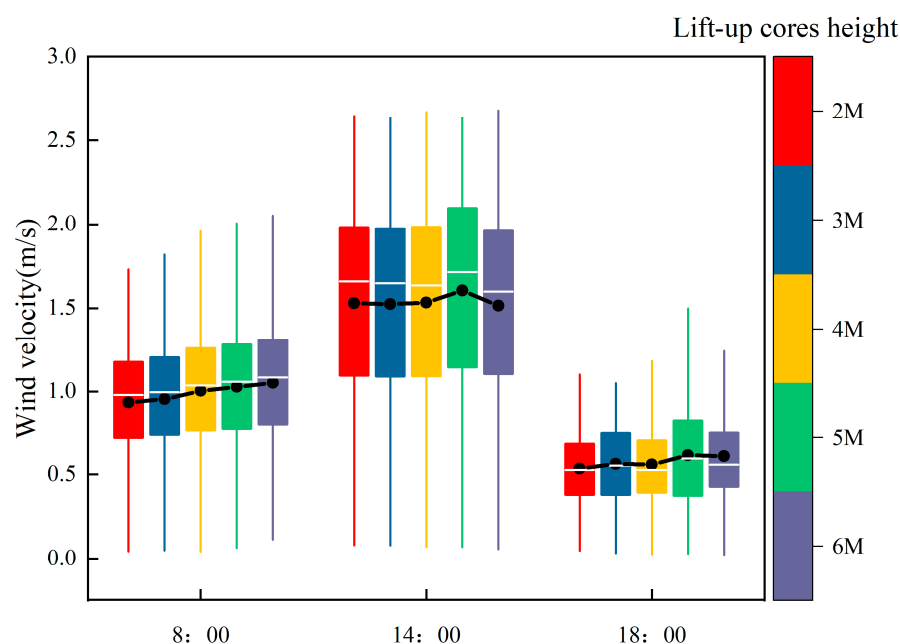


Figure 12. Wind speeds in the target area at 8:00, 14:00, and 18:00 (Different piloti height model).

From the changes in average wind speed and comfortable wind ratio, it can be found that increasing the piloti height has a certain optimization effect on the overall wind environment of the target area, because the elevation reduces the obstruction of the air in the process of circulation. However, there is a certain threshold. When the piloti height is increased to 6 m, the average wind speed and the proportion of comfortable wind in the target area can decrease to a certain extent, worsening the wind environment.

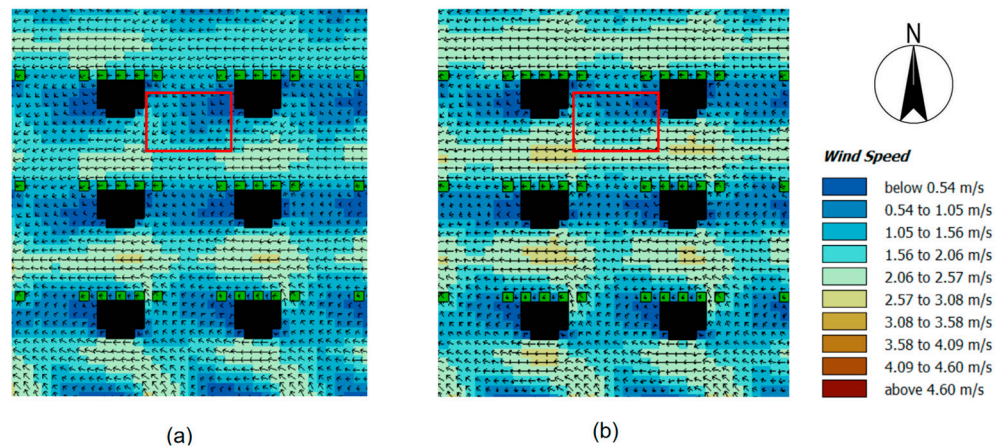


Figure 13. Vector diagram of wind speed, where (a,b) are building models with piloti heights of 6 m and 5 m, respectively.

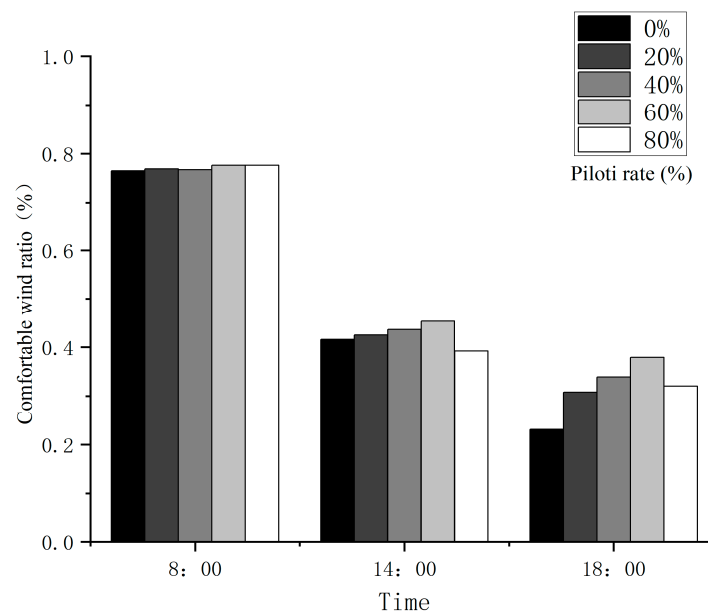


Figure 14. Schematic representation of the proportion of comfortable winds at 8:00, 14:00, and 18:00 for buildings with different piloti heights in the target area.

3.2.3. PET

The simulation results of PET for buildings with different piloti heights are shown in Figure 15. In the target and aisle areas, the changes in PET with changes in the piloti height are small, both within $0.3\text{ }^{\circ}\text{C}$. At 8:00, the increase in piloti height decreases the average PET in the target and aisle areas, while the PET increases at 14:00 and 18:00. Meanwhile, an increase in the piloti height significantly increases the lower limit of PET in the target area. At 14:00, this lower limit in the target area of buildings with a piloti height of 6 m rises by almost $5\text{ }^{\circ}\text{C}$ compared to the buildings with a piloti height of 2 m.

In the piloti area, the average PET increases with the rising piloti height, and the difference between the maximum and minimum values of PET increases significantly. At 8:00, 14:00, and 18:00, the average PETs rise by $0.46\text{ }^{\circ}\text{C}$, $0.97\text{ }^{\circ}\text{C}$, and $0.54\text{ }^{\circ}\text{C}$ for every 1 m increase in the piloti height, respectively. Meanwhile, due to the rising piloti height, the outermost PETs of the overhead region become high, which are shown as abnormal values in the box plot.

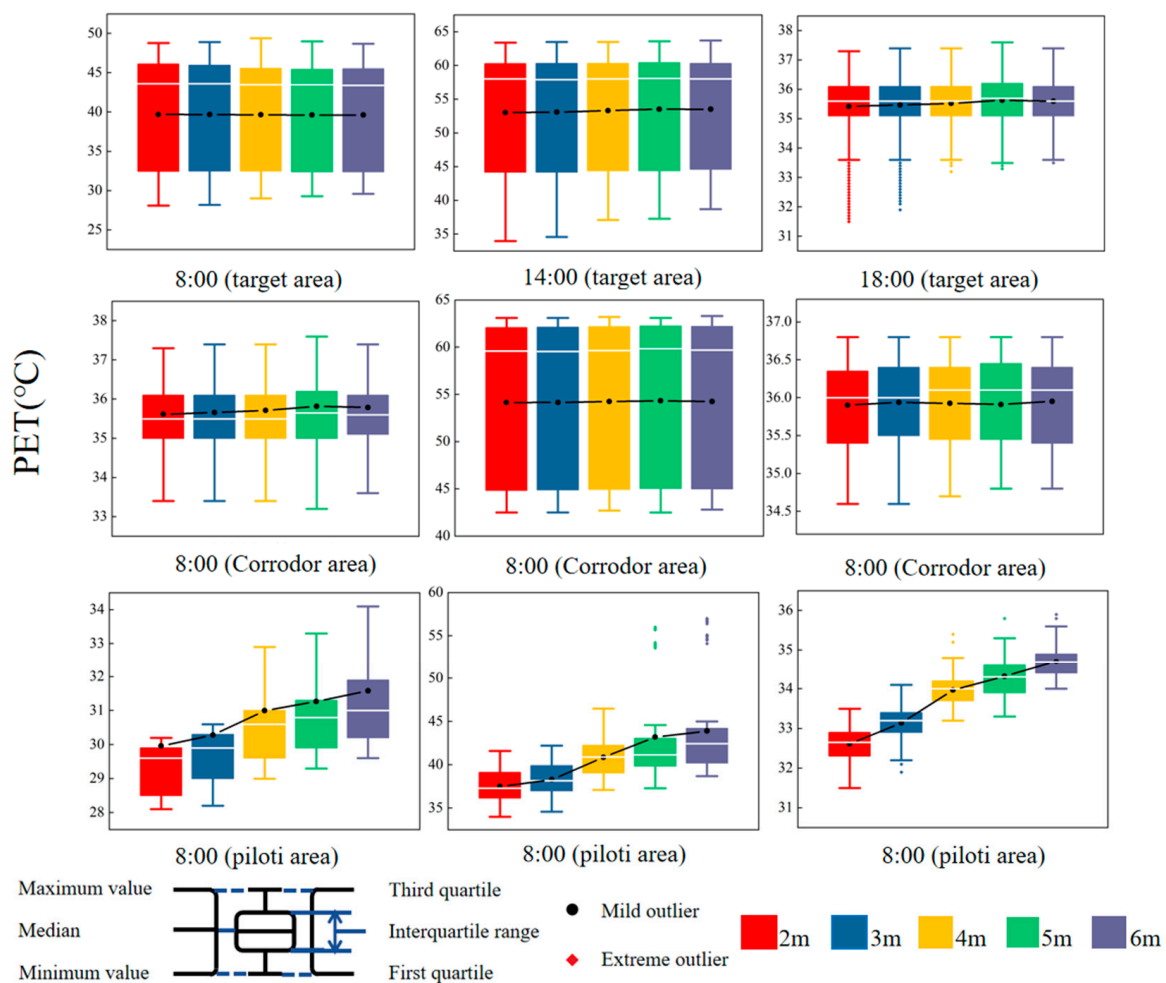


Figure 15. The 1.5 m height PET of the study area (target area, aisle area, piloti area) for buildings with different piloti heights (2 m–6 m) at different times of the day: morning (8:00), midday (14:00), nightfall (18:00).

Therefore, it can be concluded that increasing the piloti height not only increases the average PET value in the target area but also increases the lower PET limit more significantly. In summer, pedestrians tend to walk where there is greater thermal comfort, so a significant increase in the lower PET limit can lead pedestrians to feel hotter while walking. In the aisle area, the effect of piloti height on the average PET is not huge. In the piloti area, the increase in piloti height leads to a significant increase in PET at all three time points, creating an unfavorable thermal environment.

3.3. Analysis of the Impact of Different Greening Rates on the Thermal Environment in Piloti Residential Areas

3.3.1. Air Temperature

The effects of different greening rates on the air temperature are shown in Figure 16. The physical properties of vegetation such as shading and reflection lower the reception of solar radiation by the surrounding environment. At the same time, the transpiration of vegetation consumes heat and reduces the air temperature in residential areas, so the average air temperature at the pedestrian level in the target area decreases as the greening rate increases. In the target area, every 5% increase in the greening rate reduces the air temperature by 0.032 °C, 0.055 °C, and 0.04 °C at 8:00, 14:00, and 18:00, respectively.

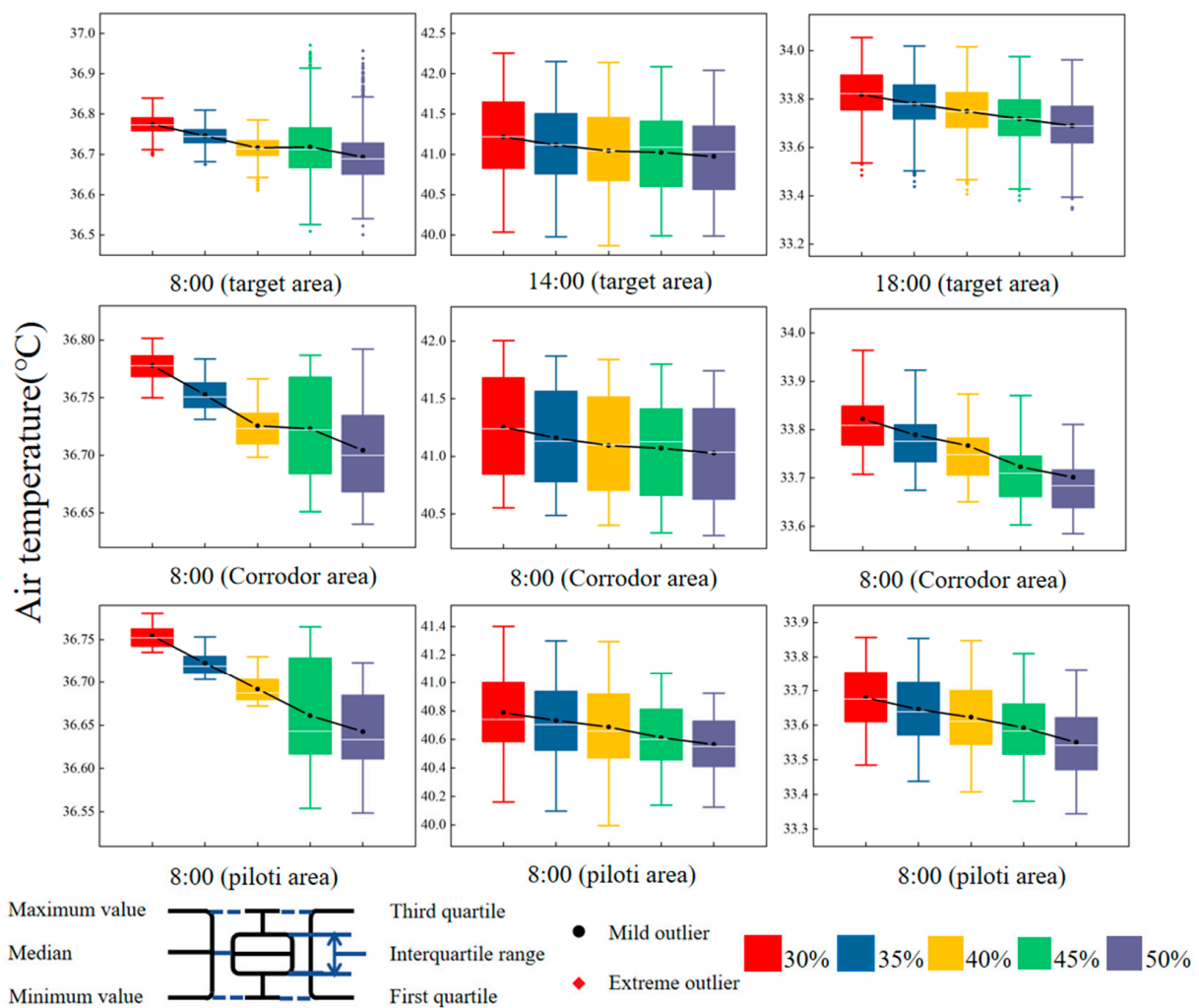


Figure 16. Average air temperature at 1.5 m height in the study area (target area, aisle area, piloti area) at different times of the day for buildings with different greening rates (30–50%): morning (8:00), midday (14:00), and nightfall (18:00).

Like the target area, the average air temperatures at the pedestrian level at 8:00, 14:00, and 18:00 decrease by 0.03 °C, 0.054 °C, and 0.016 °C in the aisle area and by 0.031 °C, 0.057 °C, and 0.0187 °C in the piloti area, respectively, as the greening rate continues to increase. Unlike the temperature changes brought about by the piloti ratio, the temperature changes brought about by the increase in greening rate are essentially the same for the target area and the aisle area. We suggest that the temperature changes from the increasing greening rate are distributed more uniformly, i.e., the average air temperature at the pedestrian level within the target area is reduced on the whole.

3.3.2. Wind Speed and Comfort Wind Ratio

The simulation results for wind speed are shown in Figure 17, from which it can be seen that the greening rate has a mitigating effect on the overall average wind speed at the pedestrian level in the target area. At 8:00, the wind speed and greening rate have a linear relationship, and for every 5% increase in greening rate, the wind speed decreases by 0.0165 m/s. At 14:00, when the greening rate varies from 30% to 40%, the wind speed decreases by 0.082 m/s for every 5% increase in greening rate; meanwhile, when the greening rate varies from 40% to 50%, the wind speed varies within a small range, decreasing by about 0.0236 m/s for every 5% increase in greening rate. At 18:00, the change in wind speed is slight because the wind speed in the target area is very low. The average

comfortable wind ratios for the models with different greening rates in the target area are shown in Figure 18. As the greening rate increases, the comfortable wind proportion decreases, but the decline is very limited.

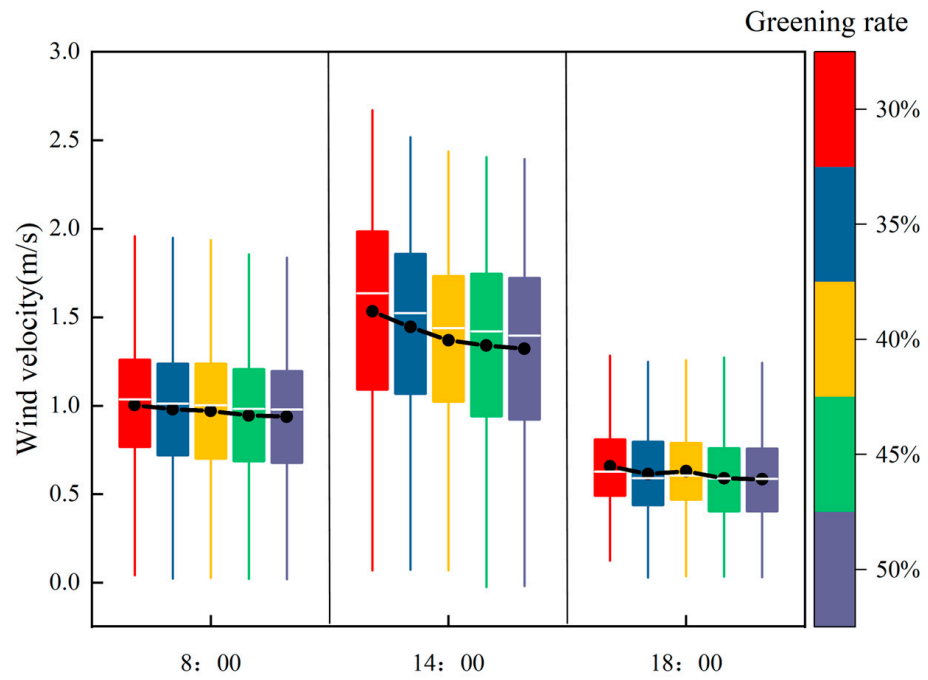


Figure 17. Wind speeds in the target area at 8:00, 14:00, and 18:00 (Different greening rate model).

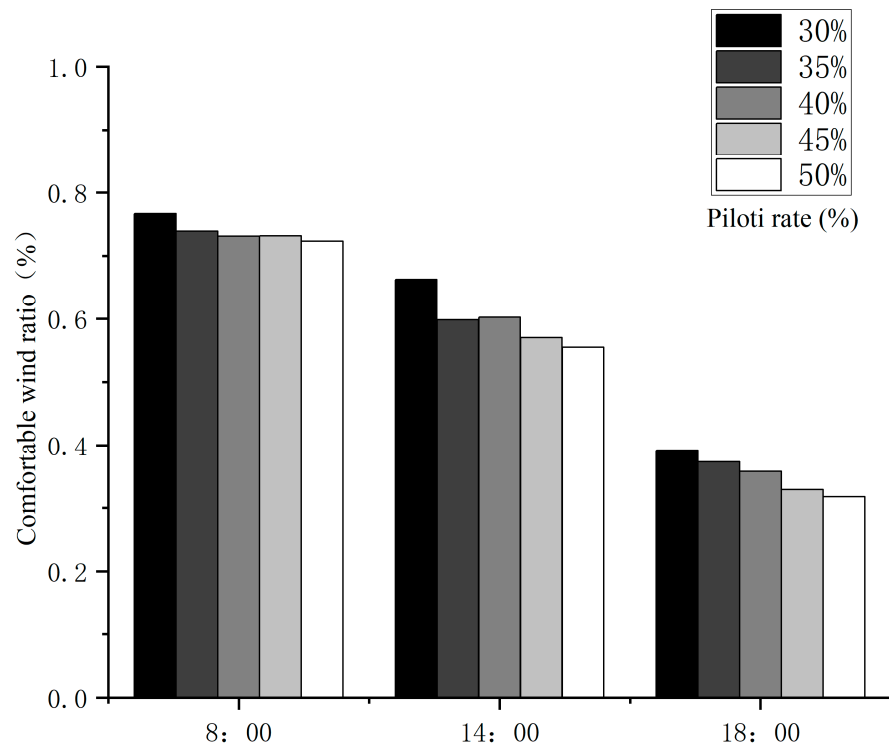


Figure 18. Histogram of the proportion of comfortable winds in the target area.

3.3.3. PET

PET box plots of buildings with different greening rates at the three time points are shown in Figure 19. An overall trend of PET decreasing with increasing greenness is shown.

At 8:00, for every 5% increase in greening rate, the PETs in the target area, aisle area, and piloti area decrease by 0.271 °C, 0.071 °C, and 0.069 °C, respectively. The average PET of the pedestrian layer in the target area demonstrates a clear change because the trees can provide shade and thus the PET of the shaded area decreases significantly. This temperature difference can reach more than 10 °C, thus lowering the average PET of the target area. Both the aisle area and the piloti area have a much slighter change in PET due to the lack of shade provided by the trees; at the same time, the upper limit of the PET decreases with the increase in the greening rate.

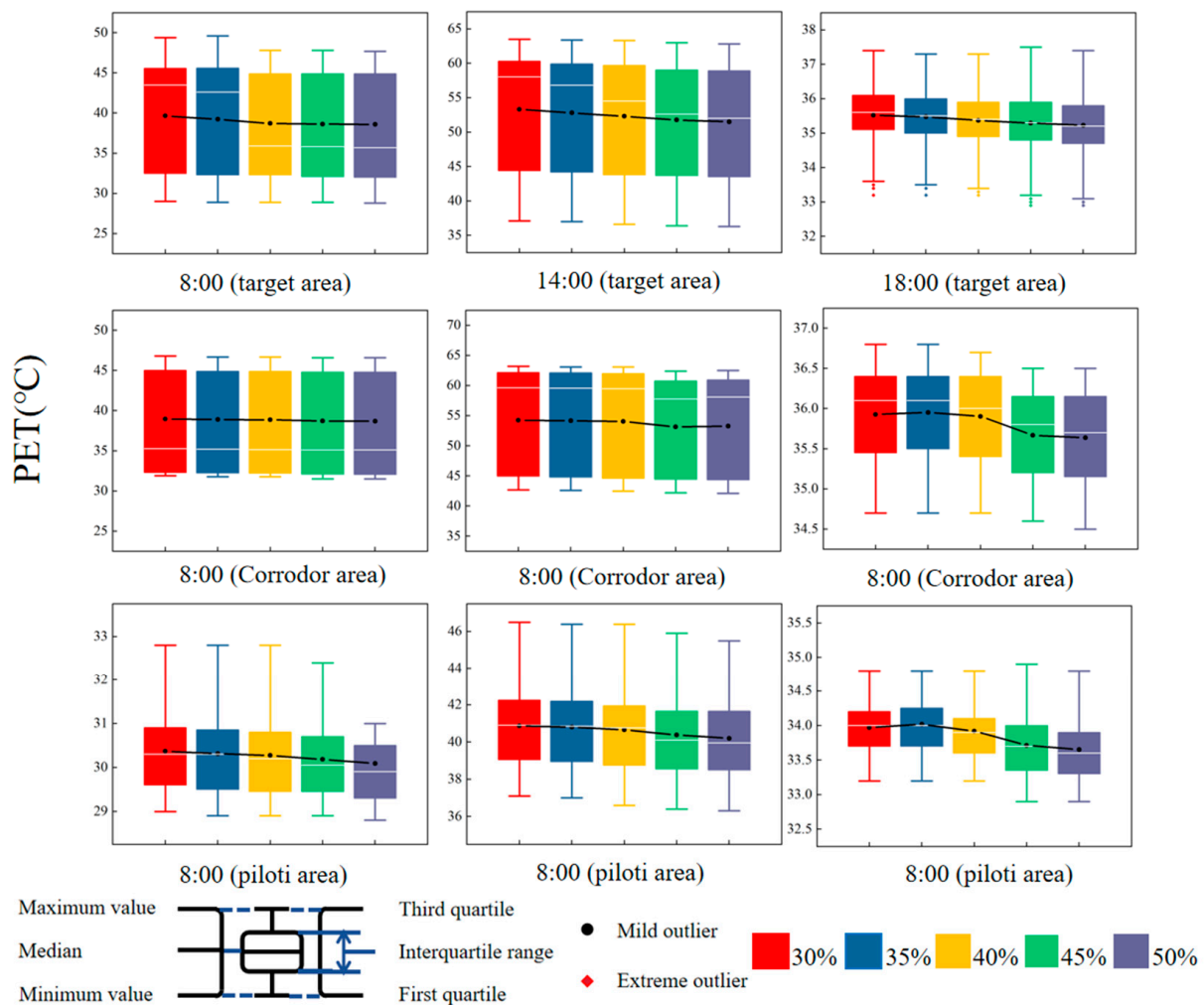


Figure 19. Average PET at 1.5 m height of the study area (target area, aisle area, piloti area) for buildings with different greening rates (30–50%) at different times of the day: morning (8:00), midday (14:00), and nightfall (18:00).

At 14:00, for every 5% increase in the greening rate, the PETs in the target and piloti areas decrease by 0.464 °C and 0.177 °C, respectively. In contrast, there is an abrupt change in the decrease in average PET in the aisle area: when the greening rate increases from 40% to 45%, this decreases by 0.9 °C; when the greening rate increases from 30% to 40%, every 5% increase in greening rate can only decrease the average PET in the aisle area by about 0.1 °C. At 18:00, there is very little change in the PET due to the decreases in the average radiant temperature and the air temperature. As the greening rate increases, for each 5%, the PETs decrease in the target, aisle, and piloti areas by 0.077 °C, 0.087 °C, and 0.094 °C, respectively.

When analyzing the PET distributions in the three study areas of the building models with different greening rates, it can be concluded that an increase in the greening rate can

reduce the average value of PET at all three time points in the three study areas, and it can reduce the upper and lower bounds of the PET to improve the thermal environment. Meanwhile, the optimization of the thermal environment through the increase in the greening rate is relatively even, and the trend is largely the same in each area. This indicates that an increase in the greening rate can optimize the thermal environment in each area. Even though the aisle area is not shaded by trees and shrubs, an increase in the greening rate can still reduce the average PET.

4. Discussion

This study generated the ideal model of a piloti residential area, which is based on the piloti ratio, piloti height, and greening rate of typical residential areas in Wuhan. Numerical simulation was adopted to investigate building models with different piloti ratios, piloti heights, and greening rates. The results showed that piloti design can support passive climate adaptability in Wuhan, a city with a climate that is hot summer and cold winter in China. In this study, after taking the area's underlay and greening factors into account, the relationships between the summer outdoor thermal environment and factors including piloti design factors and the greening rate in Wuhan were investigated by applying Envi-met software. The results provide a certain reference for other hot and humid areas with similar climates to Wuhan in summer with a certain degree of adaptability.

In this study, after conducting research on buildings with different piloti heights and piloti ratios, it was found that the combined wind comfort and thermal comfort of piloti areas was great when the piloti ratio was about 60% and the piloti height was about 5 m. Since there is a lack of design codes for piloti Residential Quarters in China, this study conducted a survey on the current architectural status of piloti Residential Quarters in Wuhan. From this, we found that the piloti height of piloti residential areas is generally around 5 m, but the piloti ratio is around 40%. Therefore, the findings presented in this paper offer a certain reference for the formulation of improved norms in the piloti residential area. And the passive piloti architectural design can improve the thermal environment of the residential area, which can reduce energy consumption. However, there are some limitations to the findings presented in this article. Firstly, due to our limited computational resources, the span of the piloti ratio varies greatly among building models with different piloti ratios. In the future, by reducing the division of the piloti ratio from 20% to 10% and the piloti height from 1 m to 0.5 m, more detailed results can be obtained. Secondly, the design of the building layout was fairly homogeneous in this case, with only rows and columns of buildings considered. Thirdly, for the greening of the residential area, we only took basic vegetation types into consideration such as shrubs, lawns, and trees.

In order to further investigate different design factors' effects on the thermal environment of the piloti residential area, research in the future should incorporate more types and arrangement forms of vegetation and architectural layouts.

5. Conclusions

The purpose of this study was to investigate the thermal environmental improvement effects of various design factors in piloti residential areas. We generated a basic model of Wuhan's piloti residential quarters following research, and we considered three design variables as affecting piloti buildings in the current situation in Wuhan (piloti ratio, piloti height, and greening rate). In total, three groups with 15 sets of models were set up. The average air temperature, PET, T_{mrt} , average wind speed, and wind comfort ratios of the target area, aisle area, and piloti area were compared in a comprehensive analysis of the outdoor thermal environment of the buildings, and the following conclusions could be drawn:

1. Improving the piloti ratio and overall greening rate of residential areas can effectively reduce the air temperature, as we found in the study area. Every 5% increase in piloti ratio and 5% increase in greening rate can decrease the air temperature by 0.076 °C and 0.058 °C at the hottest time of the day, respectively. However, an increase in pilotis

- reduces the air temperature in the study area only when it is the morning (8:00) and when the piloti height increases from 2 to 4 m, while it leads to an increase in air temperature at other time points.
2. During the daytime, an increase in the piloti ratio caused the most significant enhancement of the average PET value in the pedestrian activity area. When compared with buildings with a 20% piloti ratio, the average PET for an 80% piloti ratio decreased by 2.926 °C. Meanwhile, enhancement of the greening rate was a little less effective than changing the piloti ratio. Beyond this, an increase in piloti height led to the piloti area receiving more solar radiation and surrounding thermal radiation, which greatly affected its thermal comfort. The average PETs of the piloti area rose by 0.46 °C, 0.97 °C, and 0.54 °C for every 1 m increase in the piloti height at 8:00, 14:00, and 18:00, respectively.
 3. An increase in the piloti ratio can improve the average wind speed, but the overall effect is small and can be reversed by a change in the wind direction. An increase in the greening rate reduces the average wind speed and the proportion of comfortable wind. Meanwhile, increasing the piloti ratio and piloti height can increase the proportion of comfortable wind within a certain limit, but when the piloti rate exceeds 60% and the piloti height exceeds 5 m, the proportion of comfortable wind will be reduced.
 4. If only the piloti height is increased without providing corresponding shading measures, the average radiation temperature of the buildings in the piloti area can rise quickly. Therefore, when designing high pilotis, designers should arrange green plants to create a shading effect. These have little impact on the wind speed or the wind environment, while they significantly improve the thermal environment.

The results of this study offer a reference for the planning and design of urban residential areas with hot and wet summers. Scientific and reasonable setting of piloti design variables and the greening rate can facilitate the creation of an improved urban outdoor thermal environment and improve the thermal comfort of pedestrians.

Author Contributions: Conceptualization, Q.D. and J.L.; methodology, Q.D.; software, X.S.; resources, X.S. and J.L.; data curation, J.L.; writing—original draft preparation, J.L.; writing—review and editing, J.L. and Q.D.; visualization, Q.D. All authors have read and agreed to the published version of the manuscript.

Funding: Central-Southern China Engineering Consulting and Design Group Co., Ltd.: 2023-QT85-731.

Data Availability Statement: The data presented in this study are available on request from the corresponding author.

Conflicts of Interest: The authors declare no conflicts of interest.

Appendix A

Table A1. Terms and abbreviations used in this paper.

Abbreviations	Full Name
PET	Physiological equivalent temperature
T_{mrt}	Mean radiant temperature
T_a	Air temperature
RH	Relative humidity
RMSE	Root mean square error
MAE	Mean absolute error
MAPE	Mean absolute percentage error
d	Willmott's index of agreement

Appendix B

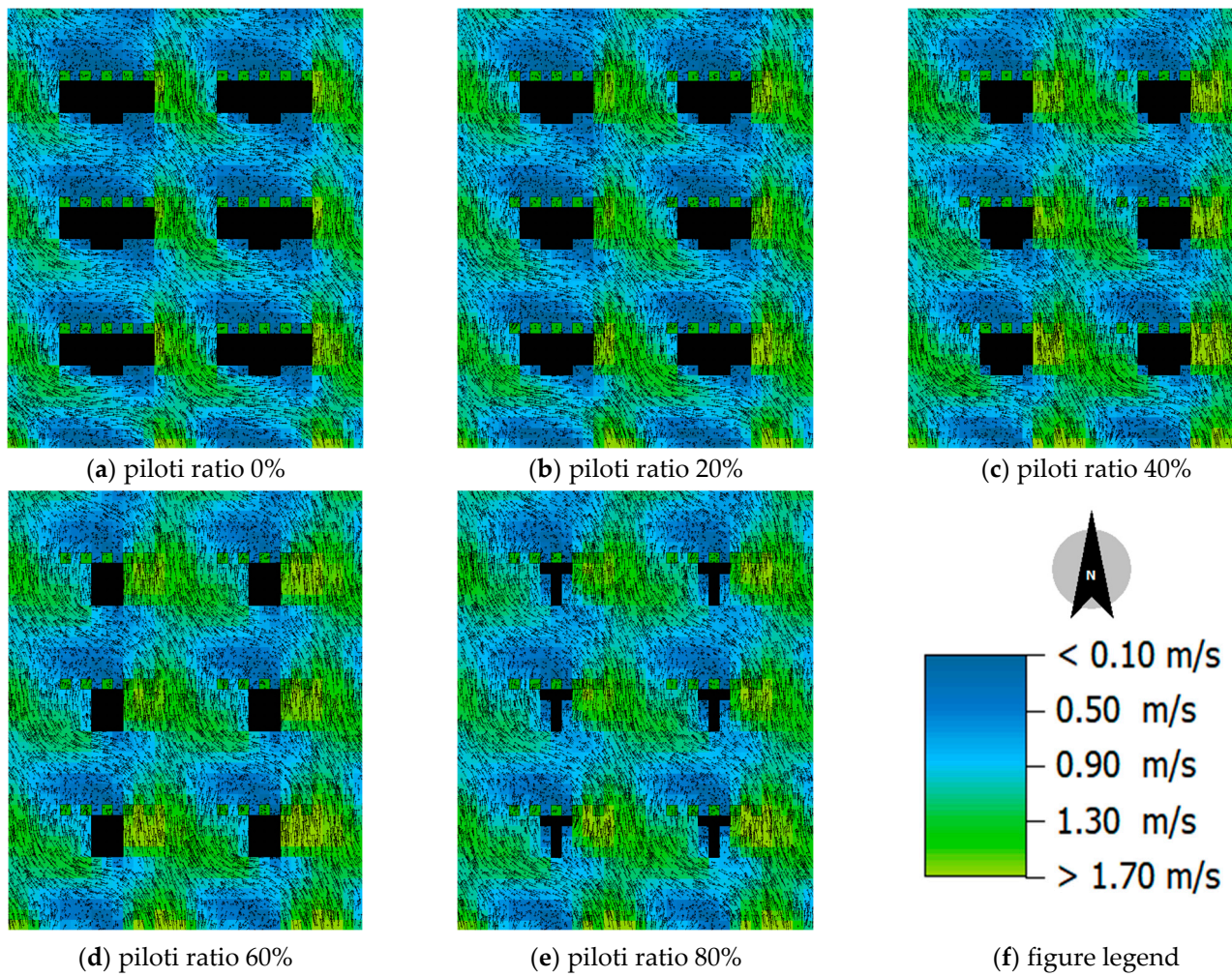


Figure A1. Vector wind speed cloud chart (8:00) of target area (Different piloti ratio model).

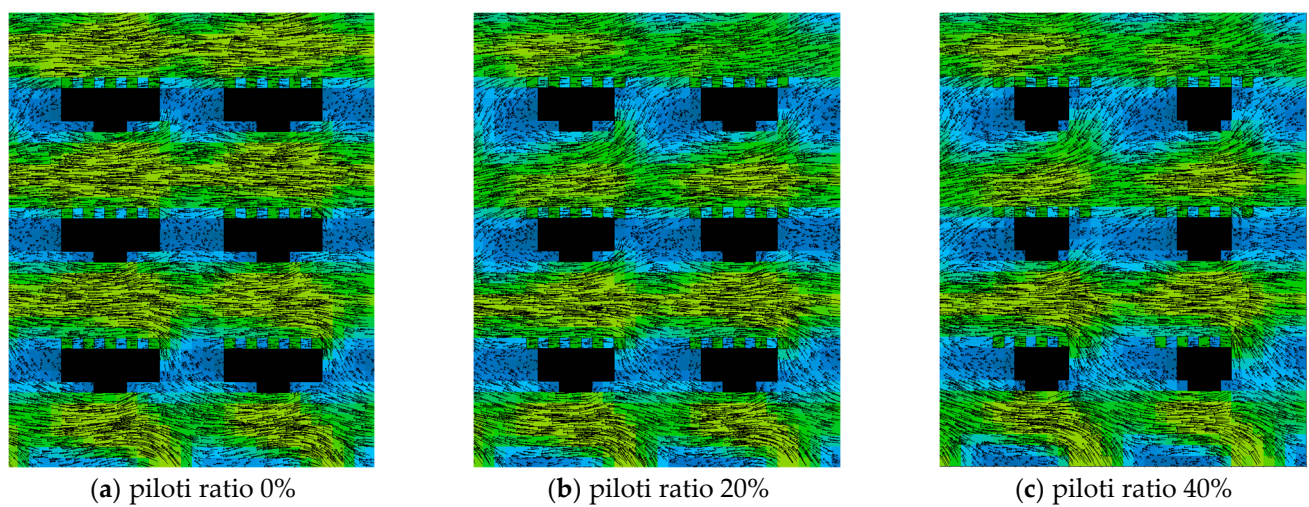


Figure A2. Cont.

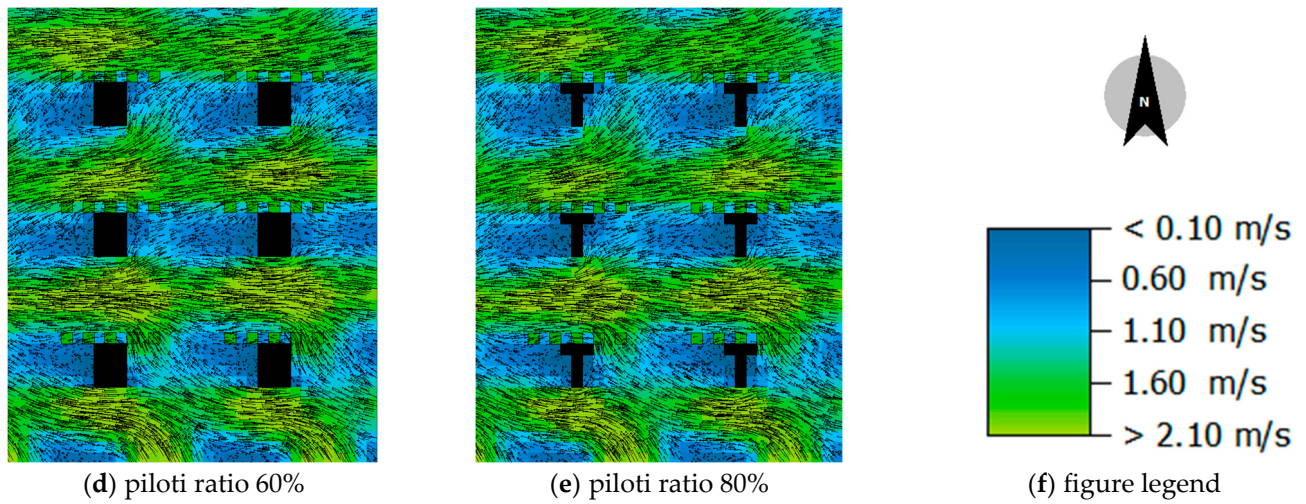


Figure A2. Vector wind speed cloud chart (14:00) of target area (Different piloti ratio model).

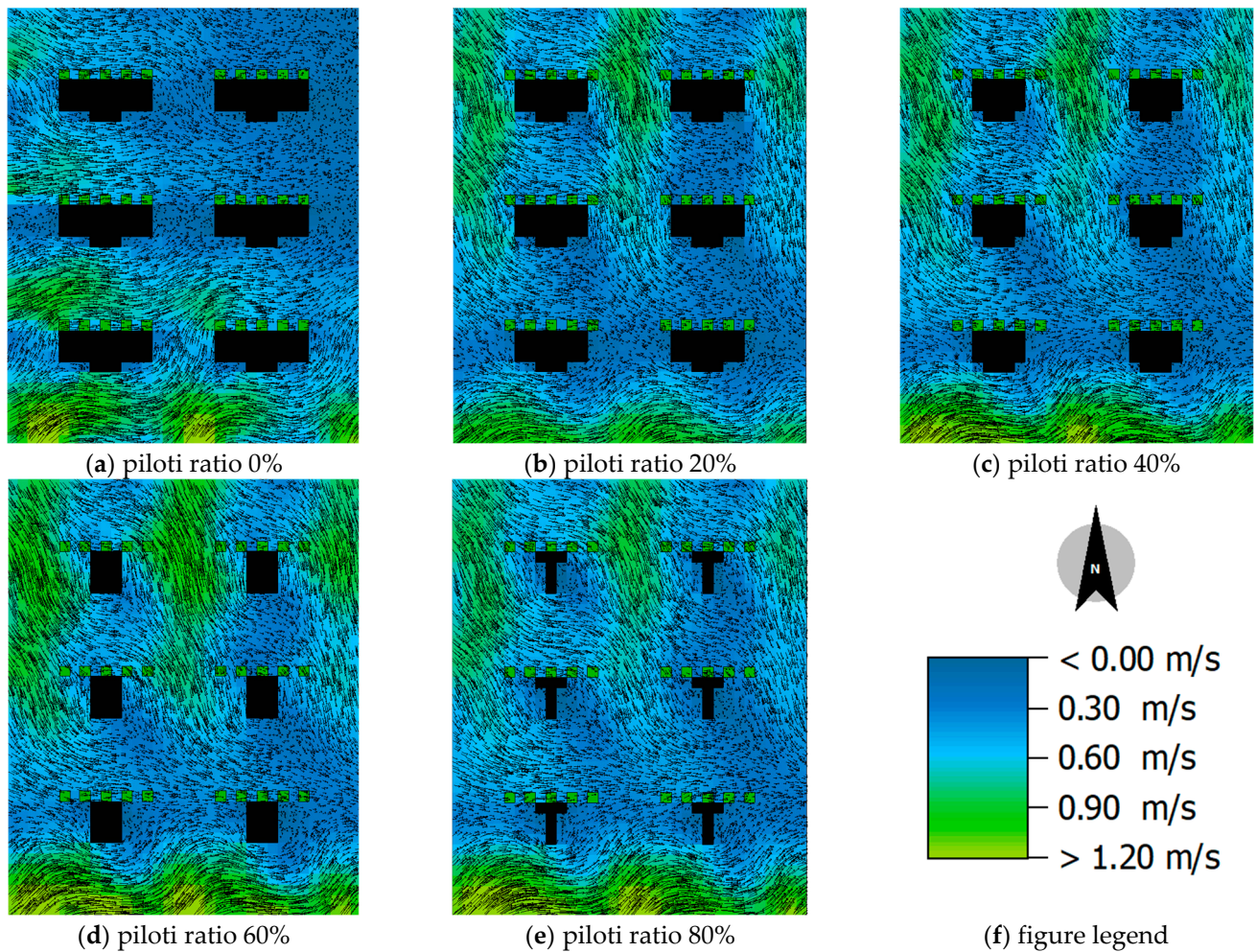


Figure A3. Vector wind speed cloud chart (18:00) of target area (Different piloti ratio model).

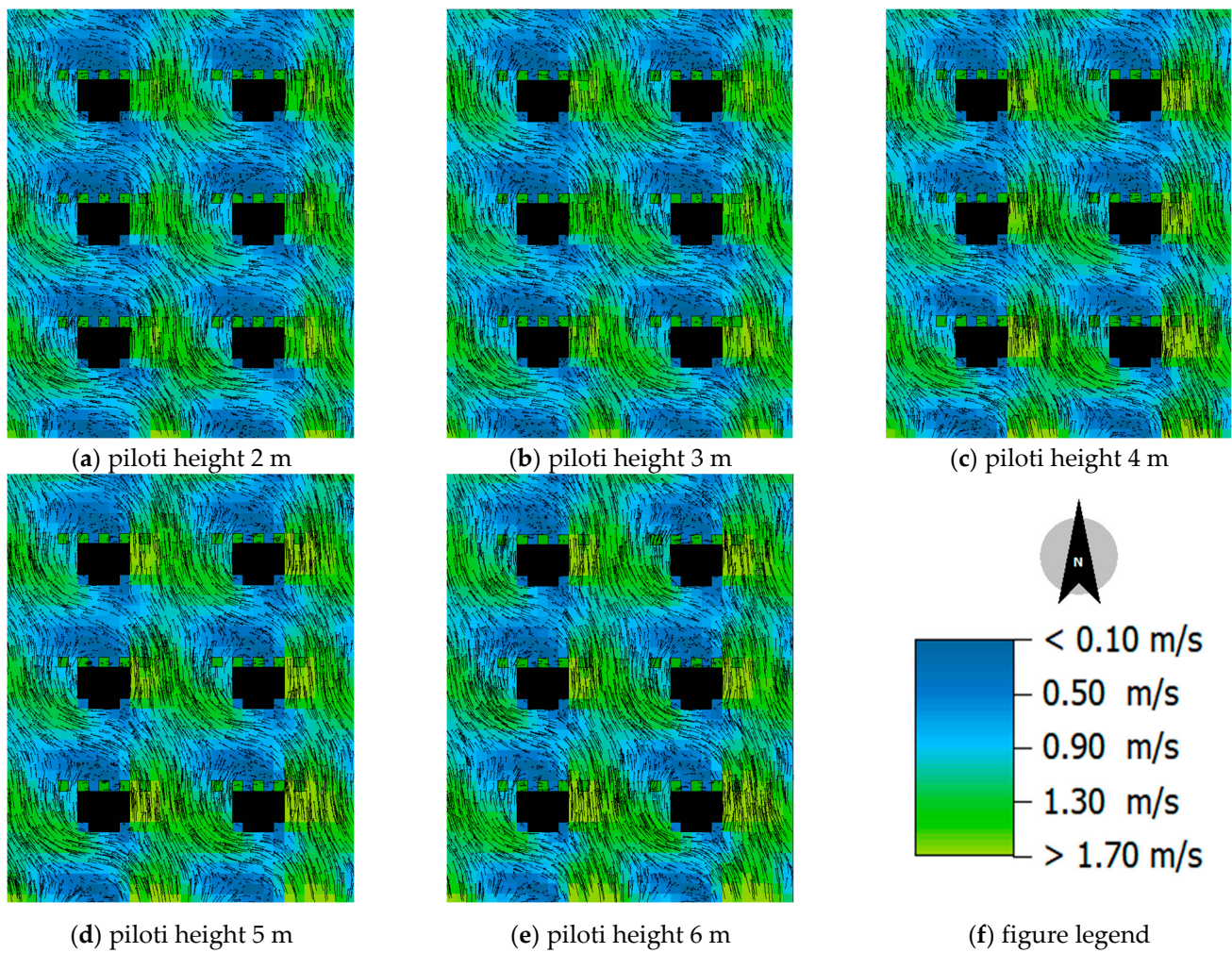


Figure A4. Vector wind speed cloud chart (8:00) of target area (Different piloti height model).

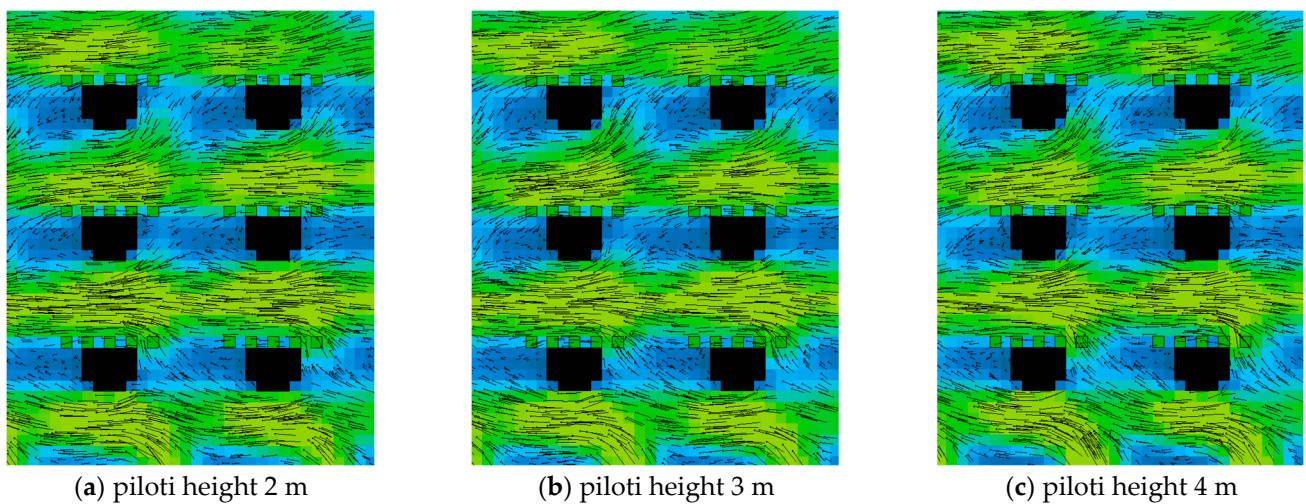


Figure A5. Cont.

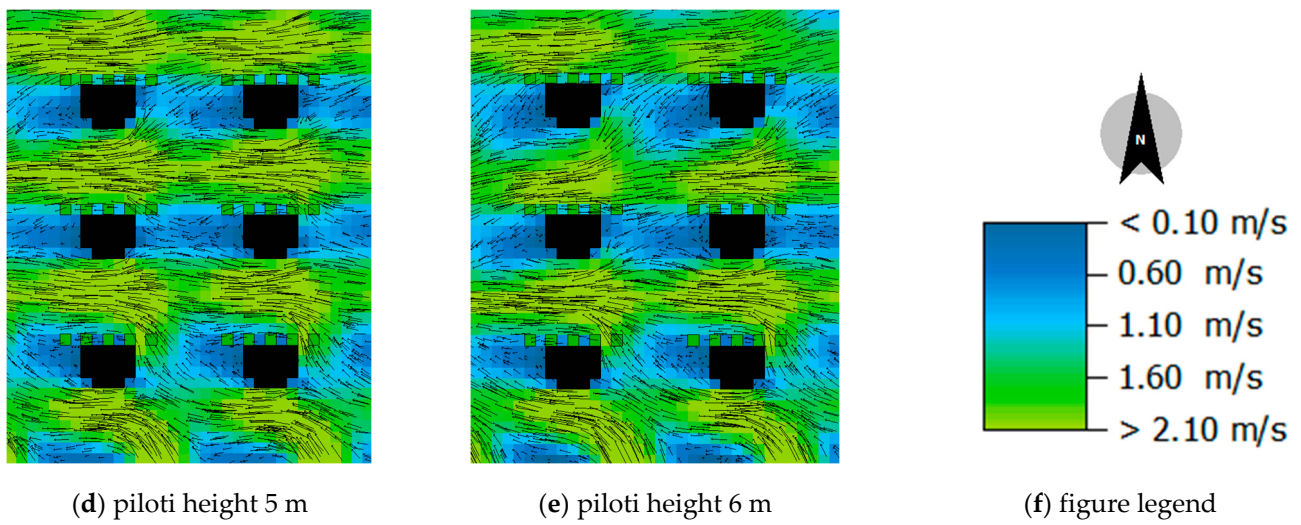


Figure A5. Vector wind speed cloud chart (14:00) of target area (Different piloti height model).

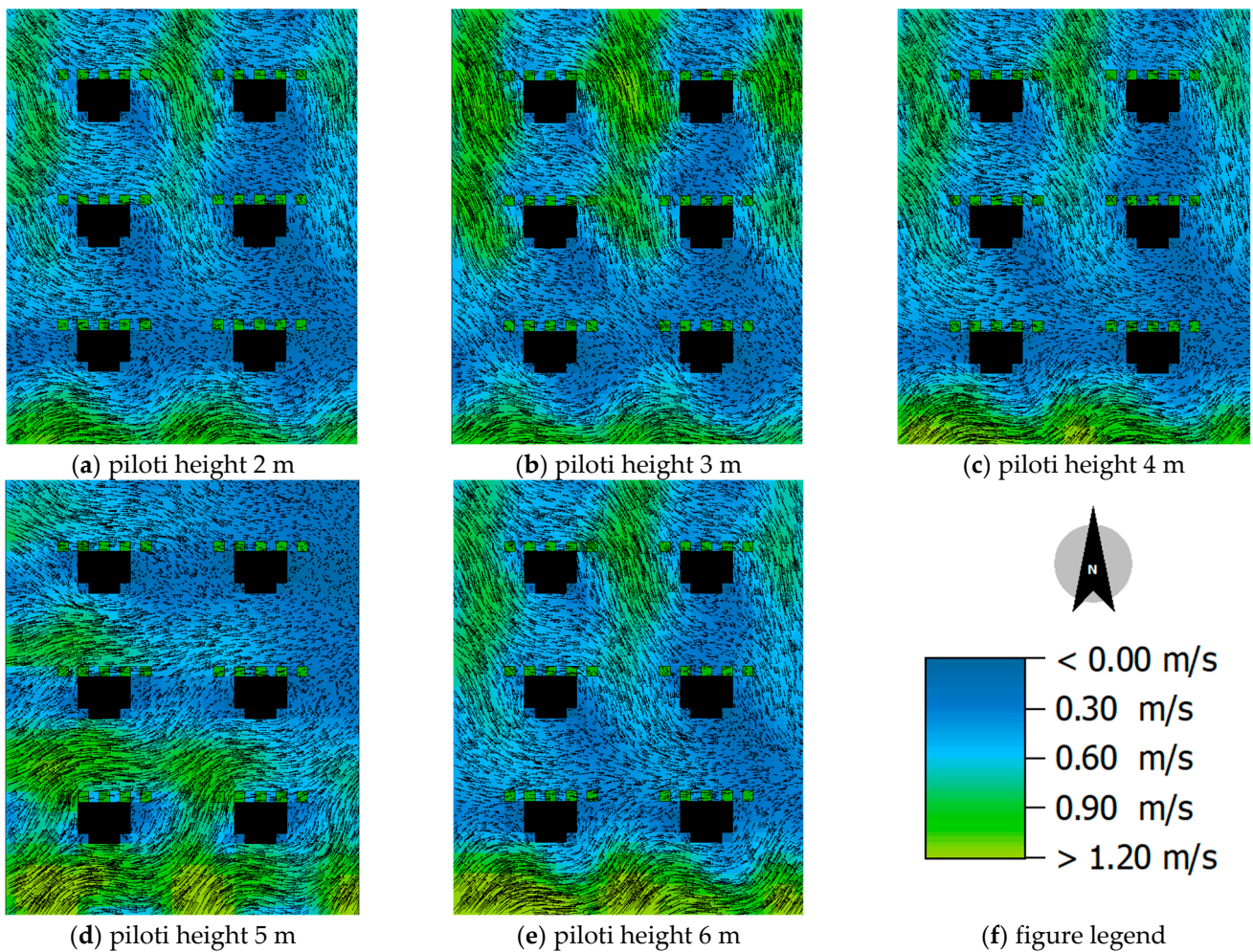


Figure A6. Vector wind speed cloud chart (18:00) of target area (Different piloti height model).

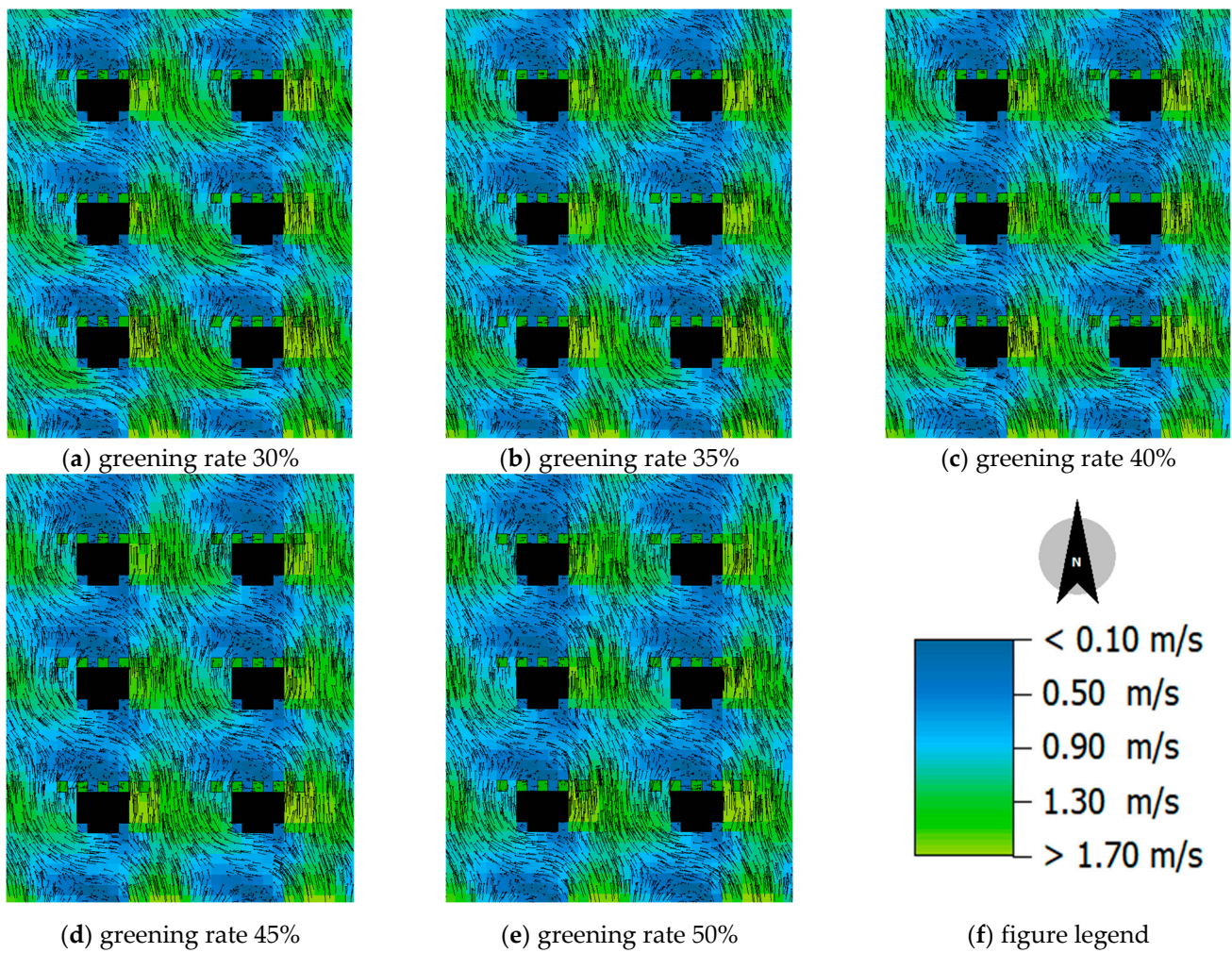


Figure A7. Vector wind speed cloud chart (8:00) of target area (Different greening rate model).

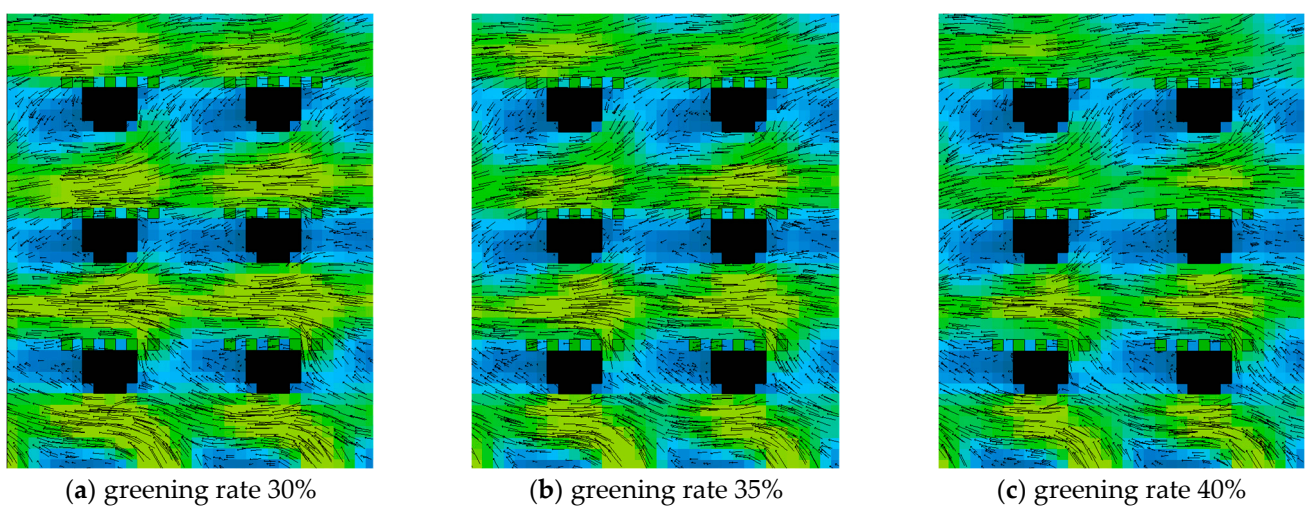


Figure A8. Cont.

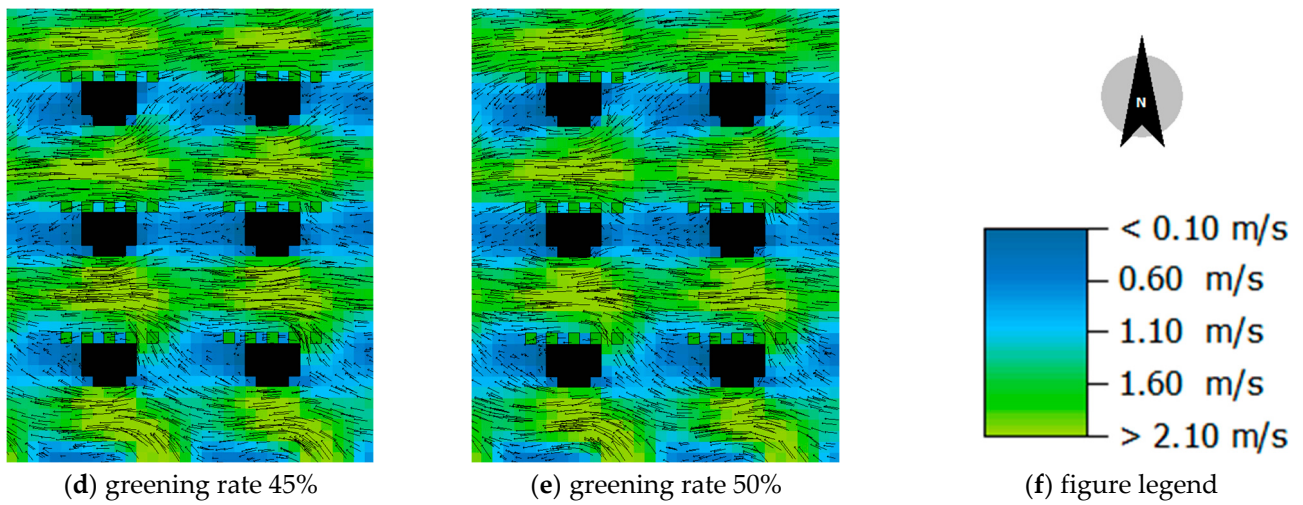


Figure A8. Vector wind speed cloud chart (14:00) of target area (Different greening rate model).

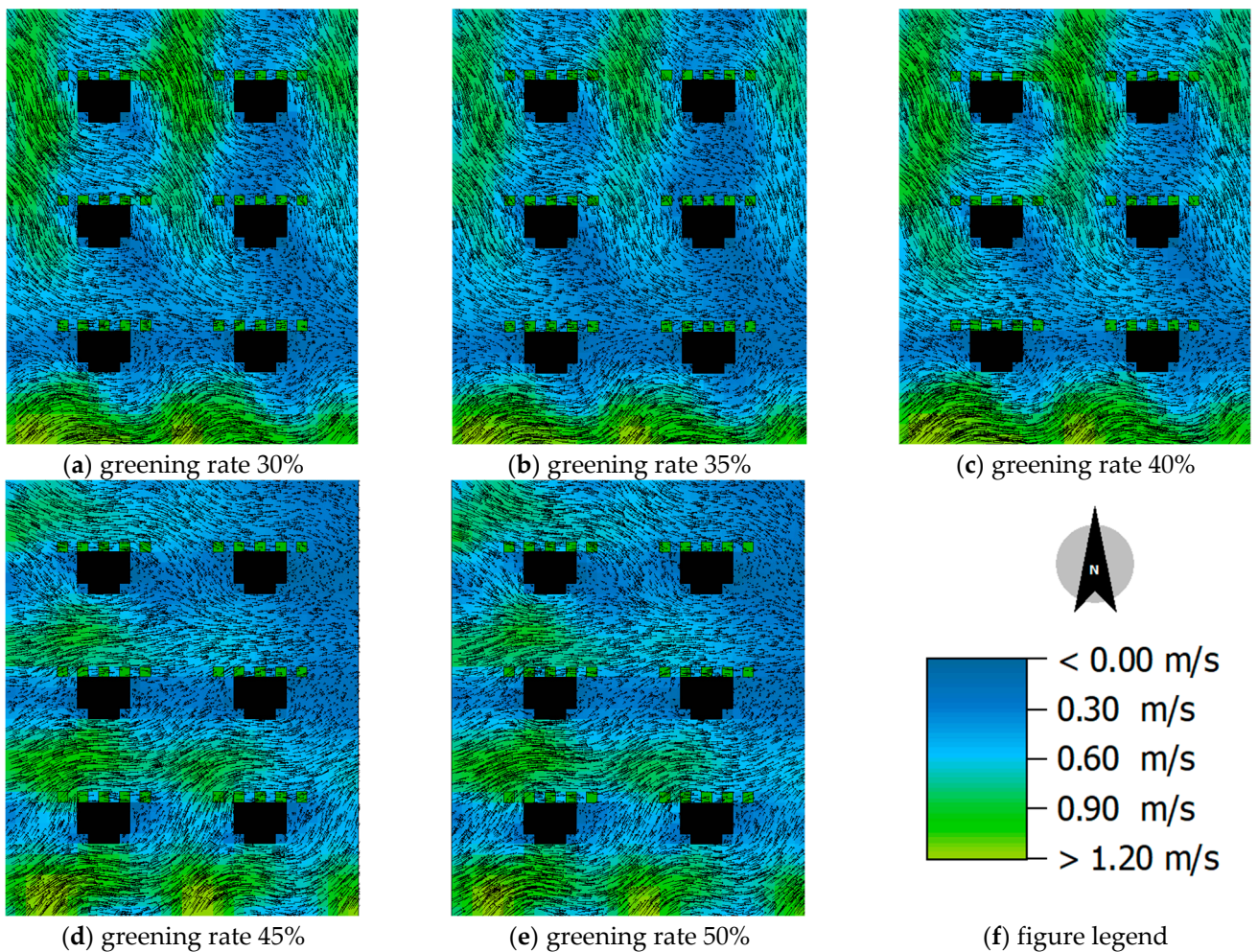


Figure A9. Vector wind speed cloud chart (18:00) of target area (Different greening rate model).

References

1. Jin, H.; Liu, Z.; Jin, Y.; Kang, J.; Liu, J. The effects of residential area building layout on outdoor wind environment at the pedestrian level in severe cold regions of China. *Sustainability* **2017**, *9*, 2310. [\[CrossRef\]](#)
2. Yu, Z.; Yang, G.; Zuo, S.; Jørgensen, G.; Koga, M.; Vejre, H. Critical review on the cooling effect of urban blue-green space: A threshold-size perspective. *Urban For. Urban Green.* **2020**, *49*, 126630. [\[CrossRef\]](#)
3. Lin, L.; Gao, T.; Luo, M.; Ge, E.; Yang, Y.; Liu, Z.; Zhao, Y.; Ning, G. Contribution of urbanization to the changes in extreme climate events in urban agglomerations across China. *Sci. Total Environ.* **2020**, *744*, 140264. [\[CrossRef\]](#)
4. Zhou, L.; Dickinson, R.E.; Tian, Y.; Fang, J.; Li, Q.; Kaufmann, R.K.; Tucker, C.J.; Myneni, R.B. Evidence for a significant urbanization effect on climate in China. *Proc. Natl. Acad. Sci. USA* **2004**, *101*, 9540–9544. [\[CrossRef\]](#)
5. Yu, Z.; Chen, T.; Yang, G.; Sun, R.; Xie, W.; Vejre, H. Quantifying seasonal and diurnal contributions of urban landscapes to heat energy dynamics. *Appl. Energy* **2020**, *264*, 114724. [\[CrossRef\]](#)
6. Tuholske, C.; Caylor, K.; Funk, C.; Verdin, A.; Sweeney, S.; Grace, K.; Peterson, P.; Evans, T. Global urban population exposure to extreme heat. *Proc. Natl. Acad. Sci. USA* **2021**, *118*, e2024792118. [\[CrossRef\]](#) [\[PubMed\]](#)
7. Watkins, R.; Palmer, J.; Kolokotroni, M.; Littlefair, P. The balance of the annual heating and cooling demand within the London urban heat island. *Build. Serv. Eng. Res. Technol.* **2002**, *23*, 207–213. [\[CrossRef\]](#)
8. Santamouris, M.; Papanikolaou, N.; Livada, I.; Koronakis, I.; Georgakis, C.; Argiriou, A.; Assimakopoulos, D. On the impact of urban climate on the energy consumption of buildings. *Sol. Energy* **2001**, *70*, 201–216. [\[CrossRef\]](#)
9. Ko, Y. Trees and vegetation for residential energy conservation: A critical review for evidence-based urban greening in North America. *Urban Forest. Urban Green.* **2018**, *34*, 318–335. [\[CrossRef\]](#)
10. Zhu, S.; Yang, Y.; Yan, Y.; Causone, F.; Jin, X.; Zhou, X.; Shi, X. An evidence-based framework for designing urban green infrastructure morphology to reduce urban building energy use in a hot-humid climate. *Build. Environ.* **2022**, *219*, 109181. [\[CrossRef\]](#)
11. Huang, J.; Zhou, C.; Zhuo, Y.; Xu, L.; Jiang, Y. Outdoor thermal environments and activities in open space: An experiment study in humid subtropical climates. *Build. Environ.* **2016**, *103*, 238–249. [\[CrossRef\]](#)
12. Gu, C.; Guan, W.; Liu, H. Chinese urbanization 2050: SD modeling and process simulation. *Sci. China Earth Sci.* **2017**, *60*, 1067–1082. [\[CrossRef\]](#)
13. Du, Y.; Mak, C.M.; Li, Y. Application of a multi-variable optimization method to determine lift-up design for optimum wind comfort. *Build. Environ.* **2018**, *131*, 242–254. [\[CrossRef\]](#)
14. Li, J.; Wang, W.; Jin, H.; Li, Y.; Bu, N. Thermal responses of people exhibiting high metabolic rates when exercising in piloti spaces in hot and humid areas. *J. Build. Eng.* **2022**, *48*, 103930. [\[CrossRef\]](#)
15. Du, Y.; Mak, C.M.; Liu, J.; Xia, Q.; Niu, J.; Kwok, K. Effects of lift-up design on pedestrian level wind comfort in different building configurations under three wind directions. *Build. Environ.* **2017**, *117*, 84–99. [\[CrossRef\]](#)
16. Huang, T.; Niu, J.; Xie, Y.; Li, J.; Mak, C.M. Assessment of “lift-up” design’s impact on thermal perceptions in the transition process from indoor to outdoor. *Sustain. Cities Soc.* **2020**, *56*, 102081. [\[CrossRef\]](#)
17. Sha, C.; Wang, X.; Lin, Y.; Fan, Y.; Chen, X.; Hang, J. The impact of urban open space and ‘lift-up’ building design on building intake fraction and daily pollutant exposure in idealized urban models. *Sci. Total Environ.* **2018**, *633*, 1314–1328. [\[CrossRef\]](#) [\[PubMed\]](#)
18. Tse, K.T.; Zhang, X.; Weerasuriya, A.U.; Li, S.W.; Kwok, K.C.; Mak, C.M.; Niu, J. Adopting ‘lift-up’ building design to improve the surrounding pedestrian-level wind environment. *Build. Environ.* **2017**, *117*, 154–165. [\[CrossRef\]](#) [\[PubMed\]](#)
19. Chen, L.; Mak, C.M. Integrated impacts of building height and upstream building on pedestrian comfort around ideal lift-up buildings in a weak wind environment. *Build. Environ.* **2021**, *200*, 107963. [\[CrossRef\]](#)
20. Lai, D.; Liu, W.; Gan, T.; Liu, K.; Chen, Q. A review of mitigating strategies to improve the thermal environment and thermal comfort in urban outdoor spaces. *Sci. Total Environ.* **2019**, *661*, 337–353. [\[CrossRef\]](#)
21. Xi, T.; Ding, J.; Jin, H.; Mochida, A. Study on the influence of piloti ratio on thermal comfort of residential blocks by local thermal comfort adaptation survey and CFD simulations. *Energy Procedia* **2017**, *134*, 712–722. [\[CrossRef\]](#)
22. Xi, T.; Li, Q.; Mochida, A.; Meng, Q. Study on the outdoor thermal environment and thermal comfort around campus clusters in subtropical urban areas. *Build. Environ.* **2012**, *52*, 162–170. [\[CrossRef\]](#)
23. Zhou, Z.; Deng, Q.; Yang, G.; Lin, Y. Quantitative study of using piloti for passive climate adaptability in a hot-summer and cold-winter city in China. *Int. J. Environ. Res. Public Health* **2018**, *15*, 2202. [\[CrossRef\]](#) [\[PubMed\]](#)
24. Chen, G.; Zhao, L.H.; Li, Q. Simulation Study on Effect of Piloti on Outdoor Thermal Environment of Campus Cluster in Guangzhou. *Appl. Mech. Mater.* **2013**, *368*, 1888–1893. [\[CrossRef\]](#)
25. Jiao, M.; Zhou, W.; Zheng, Z.; Yan, J.; Wang, J. Optimizing the shade potential of trees by accounting for landscape context. *Sustain. Cities Soc.* **2021**, *70*, 102905. [\[CrossRef\]](#)
26. Wong, N.H.; Tan, C.L.; Kolokotsa, D.D.; Takebayashi, H. Greenery as a mitigation and adaptation strategy to urban heat. *Nat. Rev. Earth Environ.* **2021**, *2*, 166–181. [\[CrossRef\]](#)
27. Yu, Z.; Zhang, J.; Yang, G. How to build a heat network to alleviate surface heat island effect? *Sustain. Cities Soc.* **2021**, *74*, 103135. [\[CrossRef\]](#)
28. Battista, G.; de Lieto Vollaro, R.; Zinzi, M. Assessment of urban overheating mitigation strategies in a square in Rome, Italy. *Sol. Energy* **2019**, *180*, 608–621. [\[CrossRef\]](#)

29. Georgescu, M.; Chow, W.T.; Wang, Z.H.; Brazel, A.; Trapido-Lurie, B.; Roth, M.; Benson-Lira, V. Prioritizing urban sustainability solutions: Coordinated approaches must incorporate scale-dependent built environment induced effects. *Environ. Res. Lett.* **2015**, *10*, 061001. [[CrossRef](#)]
30. Liu, H.; Lim, J.Y.; Thet, B.W.H.; Lai, P.Y.; Koh, W.S. Evaluating the impact of tree morphologies and planting densities on outdoor thermal comfort in tropical residential precincts in Singapore. *Build. Environ.* **2022**, *221*, 109268. [[CrossRef](#)]
31. Zhou, W.; Huang, G.; Pickett, S.T.; Wang, J.; Cadenasso, M.; McPhearson, T.; Grove, J.M.; Wang, J. Urban tree canopy has greater cooling effects in socially vulnerable communities in the US. *One Earth* **2021**, *4*, 1764–1775. [[CrossRef](#)]
32. Yang, Y.; Zhou, D.; Wang, Y.; Meng, X.; Gu, Z.; Xu, D.; Han, X. Planning method of centralized greening in high-rise residential blocks based on improvement of thermal comfort in summer. *Sustain. Cities Soc.* **2022**, *80*, 103802. [[CrossRef](#)]
33. Middel, A.; Chhetri, N.; Quay, R. Urban forestry and cool roofs: Assessment of heat mitigation strategies in Phoenix residential neighborhoods. *Urban For. Urban Green.* **2015**, *14*, 178–186. [[CrossRef](#)]
34. Lee, H.; Mayer, H.; Chen, L. Contribution of trees and grasslands to the mitigation of human heat stress in a residential district of Freiburg, Southwest Germany. *Landsc. Urban Plan.* **2016**, *148*, 37–50. [[CrossRef](#)]
35. Mayer, H.; Höpfe, P. Thermal comfort of man in different urban environments. *Theor. Appl. Climatol.* **1987**, *38*, 43–49. [[CrossRef](#)]
36. Murakami, S. Criteria for assessing wind-induced discomfort considering temperature effect. *J. Archit. Plann. Environ. Eng. AIJ* **1985**, *358*, 9–17.
37. Li, Q.; Meng, Q.L.; Zhao, L.H.; Yang, X.S.; Shu, L.F. Experimental study on outdoor thermal environment of campus building clusters in tropical climate. In Proceedings of the 7th International Conference on Urban Climate (ICUC-7), Okohama, Japan, June 29–3 July 2009.
38. Zhang, L.; Zhan, Q.; Lan, Y. Effects of the tree distribution and species on outdoor environment conditions in a hot summer and cold winter zone: A case study in Wuhan residential quarters. *Build. Environ.* **2018**, *130*, 27–39. [[CrossRef](#)]
39. Willmott, C.J. Some comments on the evaluation of model performance. *Bull. Am. Meteorol. Soc.* **1982**, *63*, 1309–1313. [[CrossRef](#)]

Disclaimer/Publisher’s Note: The statements, opinions and data contained in all publications are solely those of the individual author(s) and contributor(s) and not of MDPI and/or the editor(s). MDPI and/or the editor(s) disclaim responsibility for any injury to people or property resulting from any ideas, methods, instructions or products referred to in the content.